machines

MDPI

Article

A Bayesian FMEA-Based Method for Critical Fault Identification in Stacker-Automated Stereoscopic Warehouses

Xinyue Ma and Mengyao Gu *

School of Quality and Standardization, China Jiliang University, Hangzhou 310018, China; xinyuema0219@163.com
* Correspondence: 18A0602153@cjlu.edu.cn

Abstract: This study proposes a Bayesian failure mode and effects analysis (FMEA)-based method for identifying critical faults and guiding maintenance decisions in stacker-automated stereoscopic warehouses, addressing the limited research on whole-machine systems and the interactions among fault modes. First, the hesitant fuzzy evaluation method was utilized to assess the influences of risk factors and fault modes in a stacker-automated stereoscopic warehouse. A hesitant fuzzy design structure matrix (DSM) was then constructed to quantify their interaction strengths. Second, leveraging the interaction strengths and causal relationships between severity, detection, risk factors, and fault modes, a Bayesian network model was developed to compute the probabilities of fault modes under varying severity and detection levels. FMEA was subsequently applied to evaluate fault risks based on severity and detection scores. Following this, fault risk ranking was conducted to identify critical fault modes and formulate targeted maintenance strategies. The proposed method was validated through a case study of Company A's stacker-automated stereoscopic warehouse. The results demonstrate that the proposed approach can more objectively identify critical fault modes and develop more precise maintenance strategies. Furthermore, the Bayesian FMEA method provides a more objective and accurate reflection of fault risk rankings.

Keywords: stacker-automated stereoscopic warehouse; critical fault identification; maintenance decision-making; Bayesian FMEA



Academic Editor: Ahmed Abu-Siada

Received: 19 February 2025
Revised: 14 March 2025
Accepted: 15 March 2025
Published: 17 March 2025

Citation: Ma, X.; Gu, M. A Bayesian FMEA-Based Method for Critical Fault Identification in Stacker-Automated Stereoscopic Warehouses. *Machines* **2025**, *13*, 242. https://doi.org/10.3390/machines13030242

Copyright: © 2025 by the authors. Licensee MDPI, Basel, Switzerland. This article is an open access article distributed under the terms and conditions of the Creative Commons Attribution (CC BY) license (https://creativecommons.org/licenses/by/4.0/).

1. Introduction

In the transforming manufacturing industry, production efficiency and cost control are essential for competitiveness. The demand for intelligence and automation has grown, particularly with the rise of Industry 4.0, resulting in the rapid development of stacker-automated stereoscopic warehouses. Stacker-automated stereoscopic warehouses utilize high-level shelves and automated equipment, such as stackers, to facilitate automatic storage, handling, and goods management [1]. Integrating advanced automation with intelligent management enables precise control and real-time inventory monitoring, thereby significantly enhancing production efficiency. However, the structural complexity of stacker-automated stereoscopic warehouses can lead to various faults, and a malfunction in any component may cause unplanned downtime and disrupt the normal operations of the enterprise. Hence, detailed research on their faults is crucial to maintain production continuity and stability of enterprises.

However, current studies mainly focus on fault diagnosis and warning of stackers, and there is limited research on the entire stacker-automated stereoscopic warehouse

system and its fault maintenance strategies. A stacker-automated stereoscopic warehouse system has a complex structure, with each component serving a distinct functional role, leading to varying consequences from different fault modes. Therefore, it is essential to identify critical fault modes with significant impacts through fault risk assessments and develop appropriate maintenance strategies. Failure mode and effects analysis (FMEA) can accurately identify various types of fault modes and perform criticality assessments by calculating the Risk Priority Number (RPN). The RPN is derived from the product of the probability of occurrence (O) of each fault mode, the severity (S) of the impact, and the degree of detection (D) [2]. Compared to other methods, FMEA eliminates the cumbersome logical derivation process, reduces the difficulty and workload of analysis, and enables quick and effective fault risk assessment in practical application scenarios, such as stacker-automated stereoscopic warehouses.

However, the existing FMEA method has two main limitations: (1) It rarely considers interactions among risk factors and fault modes. While Wan Di et al. [3] addressed the interaction between risk factors and fault modes, they overlooked the effect of interactions among fault modes on the fault risk assessment results. This can lead to missing critical fault modes, thereby affecting the accuracy of risk assessment and maintenance strategy formulation. (2) Subjective methods are often used to evaluate the probability of occurrence, severity, and detection of fault modes, such as fuzzy analysis by Li et al. [4] and intuitionistic fuzzy analysis by Huang et al. [5]. The methods are susceptible to subjective factors, such as experience and preferences, and result in a high degree of arbitrariness in fault risk assessment outcomes.

To address the limitations, the study: (1) Introduces a design structure matrix (DSM) in FMEA to account for the interactions of risk factors and fault modes. The DSM is widely used to analyze interactions among system components [6]. It primarily defines a binary risk structure matrix (RSM) using 1s and 0s to indicate whether an interaction exists between pairs of interacting objects, considers the influence between two interacting objects, and uses the analytic hierarchy process (AHP) to calculate the interaction strength through pairwise comparisons of the influences [7]. However, AHP focuses on the relative importance of influences as opposed to their absolute importance, which can compromise accuracy. To improve this, a hesitant fuzzy evaluation method is introduced to evaluate the influence of two interacting objects, thereby establishing an RSM. Subsequently, the interaction strength matrix is established based on the actual ratios of influence. (2) Bayesian networks are employed for an objective assessment of fault risk levels. Bayesian networks describe the causal relationships between events, allowing for a more objective calculation of fault-mode probabilities and an intuitive representation of the interactions among risk factors and fault modes.

In summary, this study presented a Bayesian FMEA method for critical fault identification and maintenance decision-making in stacker-automated stereoscopic warehouses. Its innovations involve: (1) proposing a hesitant fuzzy DSM to improve the objectivity and reliability of fault risk assessments by considering interactions among risk factors and fault modes; and (2) the integration of Bayesian networks into FMEA to evaluate the risk levels of fault modes based on their probabilities under varying severity and detectability conditions. Additionally, this technique consists of four steps: (1) A hesitant fuzzy evaluation method was developed using an adaptive weight adjustment method and hesitant fuzzy sets to assess the influence of risk factors and fault modes in stacker-automated stereoscopic warehouses. A hesitant fuzzy DSM was then created to calculate the interaction strengths of the risk factors and fault modes. (2) A Bayesian network model was constructed with the causal relationships among the fault modes, severity, detection, and risk factors, and the probability of each fault mode at varying severity and detection levels was calculated

using the noise or gate model. (3) FMEA was employed to assess the risk level of each fault mode by combining the severity and detection scores. (4) The critical fault modes and their corresponding maintenance strategies were identified through the risk ranking of the fault modes.

2. Literature Review

2.1. Fault Study of Stacker-Automated Stereoscopic Warehouses

Researchers have extensively investigated faults in stacker-automated stereoscopic warehouses. For example, Li et al. [8] proposed a scheme that utilized ensemble empirical mode decomposition and density-based spatial clustering of noise applications to address the damage localization problem of stackers. Xue et al. [9] developed a real-time fault warning system for stackers based on S7-300 and WinCC Flexible 2007 operating environments. Bao et al. [10] established a fault tree analysis model for tunnel stackers in a tobacco factory and identified various fault modes and key factors. Mathias et al. [11] enhanced the fault diagnostic precision for stackers using an automatic model selection strategy based on dynamic simulation. Chen et al. [12] created a fault Petri net using type-2 fuzzy sets to diagnose abnormal operations in an automated stereoscopic warehouse. Gnjatovic et al. [13] utilized the original spatial reduced dynamic model to investigate the impact of constructive development parameters of stackers, such as the quality of conveyed goods, on fault coupling. Bosnjak et al. [14] examined the stacker chain links in the Kostolac open-pit mine in Serbia as their research subject, and they employed finite element analysis to diagnose the causes of faults in the stacker crawler chain links. However, the aforementioned research has limitations, as it primarily focuses on a single device and seldom considers fault maintenance strategies.

2.2. Fault Risk Assessment Methods

Existing fault risk assessment methods include fault tree analysis (FTA) [15], event tree analysis (ETA) [16], gray system theory analysis (GST) [17], Monte Carlo simulation analysis (MCS) [18], and fault mode and effects analysis (FMEA) [19]. FTA is a top-down deductive method that identifies causes and the propagation paths of faults. Qiao et al. [15] proposed a FTA model considering multiple fuzzy states for the complex causative factors of immersed and floating tunnels in the marine environment, and analyzed the causal relationships between fault modes and complex factors. However, its construction can be complex and time-consuming for large systems such as stacker-automated stereoscopic warehouses. ETA, a bottom-up inductive method, tracks the development of events from an initial occurrence to the final outcome. Renan et al. [16] combined the k-shortest path planning method with ETA to realize dynamic fault risk assessment for ship collision systems. However, it is challenging to accurately select initial events for complex equipment. Although GST assesses fault-mode risk levels using a grey model and cluster analysis, it is sensitive to data fluctuations. Complex relationships between the components and changing operating environments in stacker-automated stereoscopic warehouses can lead to data fluctuations and cause assessment results to deviate from reality. Chen et al. [17] combined GST with an object-element model to realize the construction of a fault risk assessment model for power communication networks considering both static structure and dynamic operation. MCS is a statistical technique that quantitatively assesses risks via random variable simulations. Zhang et al. [18] proposed an agent-based MCS method and applied it to scenario-simulation-based fault risk assessment of self-driving cars, which solved the problem of few fault samples of self-driving cars in natural driving environments. Although it can handle complex problems, its accuracy depends on the number of simulations and the quality of random number generation, making fault risk

assessment costly and difficult to implement in stacker-automated warehouses. FMEA systematically identifies fault modes based on their frequency, severity, and detection, allowing for risk prioritization without requiring complex diagrams, specific data quality, or simulation experiments. Hence, FMEA is particularly suitable for assessing fault risks in stacker-automated stereoscopic warehouses.

2.3. FMEA Application Research

FMEA is a crucial reliability management tool for risk assessment and fault prevention in complex systems. For example, Min et al. [20] integrated expected loss into an FMEA and developed a systematic fault risk assessment model for industrial equipment. Li et al. [4] enhanced FMEA by incorporating risk attitudes and asymmetric cost consensus, addressing resource limitations and diverse expert interests to improve the reliability of fault risk assessments in food cold chain logistics. Liu et al. [21] employed a linear programming model to minimize individual regret, determine risk factor weights in FMEA, and prioritize risks using regret theory and the TODIM method, thereby achieving a more accurate assessment of smart bracelet fault risks. Huang et al. [5] introduced intuitionistic fuzzy sets and rough number theory into FMEA to calculate expert and risk factor weights and applied the approach to assess fault risks in spark plug assembly lines. Huang et al. [22] proposed a risk assessment method that combines the acceptable risk coefficient, pessimistic–optimistic fuzzy information axiom, and FMEA to identify risk factors leading to potential fault modes in dangerous railway goods transportation systems.

Warehouses are complex systems, and the use of FMEA for risk assessment has prompted extensive research in warehouse systems, as shown in Table 1. Obviously, FMEA effectively identifies potential fault modes, assesses risk impact, and supports efficient warehouse operations.

Table 1. Application of FMEA in warehouse systems.

Author	Year	Research Target	Method	Application
Ustundag et al. [23]	2012	SCM warehouse	Fuzzy-FMEA	Fault risk assessment
Li et al. [24]	2014	Equipment warehouse	CBR-FMEA	Fault risk assessment
Salah et al. [25]	2015	Automated warehouse	Traditional FMEA	Optimized parameters for system reliability
Bevilacqua et al. [26]	2015	Pharmacy warehouse	IDEF0-FMEA	Fault risk assessment
Adriansyah et al. [27]	2018	Materials warehouse	SD-FMEA	Continuous improvement of the system of risk control
Maslowski et al. [28]	2018	Warehouse	Traditional FMEA	Find the causes of defects, to commit repair tasks
Hassan et al. [29]	2019	Cement industry warehouse	Fuzzy-analytical-hierarchy FMEA	Fault risk assessment
Indrasari et al. [30]	2021	Green SCM warehouse	Traditional FMEA	Fault risk assessment
Hsu et al. [31]	2023	Warehouse	BWM-FMEA	Fault risk assessment
Esmaeili et al. [32]	2025	Instore warehouse	DEMATEL-FMEA	Fault risk assessment

3. Hesitant Fuzzy Design Structure Matrix

3.1. Hesitant Fuzzy Evaluation of the Influence Among Interacting Objects

3.1.1. Expert Weight Calculation

Expert weights significantly affect evaluation results [33]. To further optimize the allocation of these weights, an adaptive weight adjustment method is proposed. The method

dynamically adjusts weights based on the deviation between each expert's evaluation and the group's weighted average. Hence, experts with smaller deviations receive higher weights, whereas those with larger deviations receive lower weights. The specific steps are as follows:

(1) Based on the expert background weight scoring criteria in Table 2, the background weight of the $k(k = 1, 2, \cdots, K)$th expert is calculated as

$$\omega_k = \frac{r_k}{\sum_{k=1}^{K} r_k} \tag{1}$$

where r_k denotes the total background score of the kth expert and K denotes the total number of experts.

Table 2. Expert background weight scoring criteria.

Position	Educational Level	Work Experience	Age	Familiarity Level	Score
General operators	Junior college below	1–5 years	20–25	Understand	1
Technician	Junior college	6–10 years	25–30	Between understanding and familiar	2
Junior researcher	Undergraduate	11–20 years	31–40	Familiar	3
Senior researcher	Master	20–30 years	41–50	Between familiar and very familiar	4
Senior expert	Doctor	30–40 years	50–60	Very familiar	5

(2) Based on the background weight ω_k of the kth expert, their deviation amount is calculated using the hesitant fuzzy Euclidean distance method [34] as

$$H_k = \sqrt{\sum_{q=1}^{Q} {d_{kq}}^2} \tag{2}$$

$$d_{kq} = \sqrt{\frac{1}{h}\sum_{\lambda=1}^{h} \left(e_{kq}^{\lambda} - e_q^{\lambda})^2\right.} \tag{3}$$

Here, e_{kq} denotes the evaluation value of the kth expert about the influence between the $q(q = 1, 2, \cdots, Q)$th pair of interacting objects, and e_q is its group's weighted average. e_{kq}^{λ} and e_q^{λ} denote the λth value in hesitant fuzzy numbers e_{kq} and e_q, respectively. In addition, h denotes the number of values in one hesitant fuzzy number, and d_{kq} denotes the difference between the evaluation value of the kth expert and the group's weighted average about the influence between the qth pair of interacting objects, and Q denotes the total logarithm of interacting objects.

(3) The deviation amount H_k of the kth expert is standardized and normalized to obtain the deviation of the kth expert as

$$T_k = \begin{cases} \frac{f(H_k)}{\sum_{k=1}^{K} f(H_k)}, H_k \neq 0 \\ 0, H_k = 0 \end{cases} \tag{4}$$

$$f(H_k) = \begin{cases} -\frac{1}{ln\frac{H_k}{\sum_{k=1}^{K} H_k}}, H_k \in (0, +\infty) \\ 0, H_k = 0 \end{cases} \tag{5}$$

where $f(H_k)$ denotes the standardized deviation amount of the kth expert.

(4) The deviation T_k of the kth expert is preprocessed and normalized to obtain the weight influencing factor of the kth expert as

$$\mu_k = \begin{cases} \frac{g(T_k)}{\sum_{k=1}^{K} g(T_k)}, T_k \neq 0 \\ +\infty, T_k = 0 \end{cases} \tag{6}$$

$$g(T_k) = \begin{cases} \frac{1}{e^{T_k}-1}, T_k \in (0,1) \\ +\infty, T_k = 0 \end{cases} \tag{7}$$

where $g(T_k)$ denotes the preprocessed deviation of the kth expert.

(5) The final weight of the kth expert is calculated based on its weight-influencing factor μ_k. Repeat steps one to five until the expert weights remain unchanged. Finally, the final weight of the kth expert is obtained after the pth adjustment as

$$\omega_k^{(p)} = \frac{\omega_k \times \mu_k^{(p)}}{\sum_{k=1}^{K}\left(\omega_k \times \mu_k^{(p)}\right)} \tag{8}$$

3.1.2. Influence Calculation

The influence of each pair of interacting objects was calculated based on the final expert weights and expert evaluation set. The steps were as follows:

(1) The risk-averse theory [35] states that the expert evaluation set is expanded by adding the minimum element until all sets are equal in length, after which they are normalized to obtain the evaluation matrix of the K experts as

$$A = \begin{bmatrix} \left(\frac{a_{111}}{\eta}, \frac{a_{112}}{\eta}, \cdots, \frac{a_{11\alpha}}{\eta}\right) & \left(\frac{a_{211}}{\eta}, \frac{a_{212}}{\eta}, \cdots, \frac{a_{21\alpha}}{\eta}\right) & \cdots & \left(\frac{a_{K11}}{\eta}, \frac{a_{K12}}{\eta}, \cdots, \frac{a_{K1\alpha}}{\eta}\right) \\ \left(\frac{a_{121}}{\eta}, \frac{a_{122}}{\eta}, \cdots, \frac{a_{12\alpha}}{\eta}\right) & \left(\frac{a_{221}}{\eta}, \frac{a_{222}}{\eta}, \cdots, \frac{a_{22\alpha}}{\eta}\right) & \cdots & \left(\frac{a_{K21}}{\eta}, \frac{a_{K22}}{\eta}, \cdots, \frac{a_{K2\alpha}}{\eta}\right) \\ \vdots & \vdots & \ddots & \vdots \\ \left(\frac{a_{1Q1}}{\eta}, \frac{a_{1Q2}}{\eta}, \cdots, \frac{a_{1Q\alpha}}{\eta}\right) & \left(\frac{a_{2Q1}}{\eta}, \frac{a_{2Q2}}{\eta}, \cdots, \frac{a_{2Q\alpha}}{\eta}\right) & \cdots & \left(\frac{a_{KQ1}}{\eta}, \frac{a_{KQ2}}{\eta}, \cdots, \frac{a_{KQ\alpha}}{\eta}\right) \end{bmatrix} \tag{9}$$

where η denotes the maximum length of all the evaluation sets and $a_{kq\delta}$ denotes the number of $\delta(\delta = 1, 2, \cdots, \alpha)$ evaluation levels in the evaluation set of the kth expert on the influence of the qth pair of interacting objects.

(2) Based on the final weight $\omega_k^{(p)}$ of the kth expert after the pth adjustment, the comprehensive evaluation matrix B is obtained using the weighted average method as

$$B = \begin{bmatrix} \frac{a_{111}}{\eta}\omega_1^{(p)} + \frac{a_{211}}{\eta}\omega_2^{(p)} + \cdots + \frac{a_{K11}}{\eta}\omega_K^{(p)} & \frac{a_{112}}{\eta}\omega_1^{(p)} + \frac{a_{212}}{\eta}\omega_2^{(p)} + \cdots + \frac{a_{K12}}{\eta}\omega_K^{(p)} & \cdots & \frac{a_{11\alpha}}{\eta}\omega_1^{(p)} + \frac{a_{21\alpha}}{\eta}\omega_2^{(p)} + \cdots + \frac{a_{K1\alpha}}{\eta}\omega_K^{(p)} \\ \frac{a_{121}}{\eta}\omega_1^{(p)} + \frac{a_{221}}{\eta}\omega_2^{(p)} + \cdots + \frac{a_{K21}}{\eta}\omega_K^{(p)} & \frac{a_{122}}{\eta}\omega_1^{(p)} + \frac{a_{222}}{\eta}\omega_2^{(p)} + \cdots + \frac{a_{K22}}{\eta}\omega_K^{(p)} & \cdots & \frac{a_{12\alpha}}{\eta}\omega_1^{(p)} + \frac{a_{22\alpha}}{\eta}\omega_2^{(p)} + \cdots + \frac{a_{K2\alpha}}{\eta}\omega_K^{(p)} \\ \vdots & \vdots & \ddots & \vdots \\ \frac{a_{1Q1}}{\eta}\omega_1^{(p)} + \frac{a_{2Q1}}{\eta}\omega_2^{(p)} + \cdots + \frac{a_{KQ1}}{\eta}\omega_K^{(p)} & \frac{a_{1Q2}}{\eta}\omega_1^{(p)} + \frac{a_{2Q2}}{\eta}\omega_2^{(p)} + \cdots + \frac{a_{KQ2}}{\eta}\omega_K^{(p)} & \cdots & \frac{a_{1Q\alpha}}{\eta}\omega_1^{(p)} + \frac{a_{2Q\alpha}}{\eta}\omega_2^{(p)} + \cdots + \frac{a_{KQ\alpha}}{\eta}\omega_K^{(p)} \end{bmatrix} \tag{10}$$

where $\left(\frac{a_{1q\delta}}{\eta}\omega_1^{(p)} + \frac{a_{2q\delta}}{\eta}\omega_2^{(p)} + \cdots + \frac{a_{Kq\delta}}{\eta}\omega_K^{(p)}\right)$ denotes the membership grade of the influence between the qth pair of interacting objects and the δth evaluation level.

(3) When combined with the trapezoidal fuzzy number matrix $Y = \begin{pmatrix} y_1 & y_2 & \cdots & y_\alpha \end{pmatrix}^T$, the final evaluation matrix is calculated as

$$C = \begin{bmatrix} \left(\frac{a_{111}}{\eta}\omega_1^{(p)} + \frac{a_{211}}{\eta}\omega_2^{(p)} + \cdots + \frac{a_{K11}}{\eta}\omega_K^{(p)}\right)y_1 + \left(\frac{a_{112}}{\eta}\omega_1^{(p)} + \frac{a_{212}}{\eta}\omega_2^{(p)} + \cdots + \frac{a_{K12}}{\eta}\omega_K^{(p)}\right)y_2 + \cdots + \left(\frac{a_{11\alpha}}{\eta}\omega_1^{(p)} + \frac{a_{21\alpha}}{\eta}\omega_2^{(p)} + \cdots + \frac{a_{K1\alpha}}{\eta}\omega_K^{(p)}\right)y_\alpha \\ \left(\frac{a_{121}}{\eta}\omega_1^{(p)} + \frac{a_{221}}{\eta}\omega_2^{(p)} + \cdots + \frac{a_{K21}}{\eta}\omega_K^{(p)}\right)y_1 + \left(\frac{a_{122}}{\eta}\omega_1^{(p)} + \frac{a_{222}}{\eta}\omega_2^{(p)} + \cdots + \frac{a_{K22}}{\eta}\omega_K^{(p)}\right)y_2 + \cdots + \left(\frac{a_{12\alpha}}{\eta}\omega_1^{(p)} + \frac{a_{22\alpha}}{\eta}\omega_2^{(p)} + \cdots + \frac{a_{K2\alpha}}{\eta}\omega_K^{(p)}\right)y_\alpha \\ \vdots \\ \left(\frac{a_{1Q1}}{\eta}\omega_1^{(p)} + \frac{a_{2Q1}}{\eta}\omega_2^{(p)} + \cdots + \frac{a_{KQ1}}{\eta}\omega_K^{(p)}\right)y_1 + \left(\frac{a_{1Q2}}{\eta}\omega_1^{(p)} + \frac{a_{2Q2}}{\eta}\omega_2^{(p)} + \cdots + \frac{a_{KQ2}}{\eta}\omega_K^{(p)}\right)y_2 + \cdots + \left(\frac{a_{1Q\alpha}}{\eta}\omega_1^{(p)} + \frac{a_{2Q\alpha}}{\eta}\omega_2^{(p)} + \cdots + \frac{a_{KQ\alpha}}{\eta}\omega_K^{(p)}\right)y_\alpha \end{bmatrix} \tag{11}$$

where y_δ denotes the trapezoidal fuzzy number of each evaluation level and all elements in C are fuzzy numbers. The final evaluation matrix C was then deblurred [36] to obtain the final influence between each pair of interacting objects.

3.2. Interaction Strength Calculation Method

By combining the final influence w_{ij} of the jth evaluation object with the ith evaluation object, the risk structure matrix $RSM = \begin{bmatrix} w_{11} & w_{12} & \cdots & w_{1I} \\ w_{21} & w_{22} & \cdots & w_{2I} \\ \vdots & \vdots & \ddots & \vdots \\ w_{I1} & w_{I2} & \cdots & w_{II} \end{bmatrix}$ is obtained, and I denotes the number of evaluated objects. The DSM is then used to calculate the interaction strength between each pair of interacting objects. The specific steps are as follows:

(1) The related evaluation objects of the ith evaluation object are decomposed into two parts. One part forms the reason vector $BCV_i = \begin{bmatrix} w_{i1} & w_{i2} & \cdots & w_{iI} \end{bmatrix}$, which represents evaluation objects that may affect the ith evaluation object. The other part forms the influence vector $BEV_i = \begin{bmatrix} w_{1i} \\ w_{2i} \\ \vdots \\ w_{Ii} \end{bmatrix}$, representing evaluation objects that may be affected by the ith evaluation object.

(2) After vector decomposition, row and column comparisons of the ith evaluation object are conducted. Row comparison assesses the influence from objects that affect the ith evaluation object, while column comparison evaluates the influence on objects the ith evaluation object affects. Thus, the causal and influence interaction comparison matrices of the ith evaluation object are, respectively, formed as

$$CCM_i = \begin{bmatrix} 1 & \cdots & \frac{w_{i1}}{w_{i(i-1)}} & \frac{w_{i1}}{w_{i(i+1)}} & \cdots & \frac{w_{i1}}{w_{iI}} \\ \vdots & \ddots & \vdots & \vdots & \ddots & \vdots \\ \frac{w_{i(i-1)}}{w_{i1}} & \cdots & 1 & \frac{w_{i(i-1)}}{w_{i(i+1)}} & \cdots & \frac{w_{i(i-1)}}{w_{iI}} \\ \frac{w_{i(i+1)}}{w_{i1}} & \cdots & \frac{w_{i(i+1)}}{w_{i(i-1)}} & 1 & \cdots & \frac{w_{i(i+1)}}{w_{iI}} \\ \vdots & \ddots & \vdots & \vdots & \ddots & \vdots \\ \frac{w_{iI}}{w_{i1}} & \cdots & \frac{w_{iI}}{w_{i(i-1)}} & \frac{w_{iI}}{w_{i(i+1)}} & \cdots & 1 \end{bmatrix} \tag{12}$$

$$ECM_i = \begin{bmatrix} 1 & \cdots & \frac{w_{1i}}{w_{(i-1)i}} & \frac{w_{1i}}{w_{(i+1)i}} & \cdots & \frac{w_{1i}}{w_{Ii}} \\ \vdots & \ddots & \vdots & \vdots & \ddots & \vdots \\ \frac{w_{(i-1)i}}{w_{1i}} & \cdots & 1 & \frac{w_{(i-1)i}}{w_{(i+1)i}} & \cdots & \frac{w_{(i-1)i}}{w_{Ii}} \\ \frac{w_{(i+1)i}}{w_{1i}} & \cdots & \frac{w_{(i+1)i}}{w_{(i-1)i}} & 1 & \cdots & \frac{w_{(i+1)i}}{w_{Ii}} \\ \vdots & \ddots & \vdots & \vdots & \ddots & \vdots \\ \frac{w_{Ii}}{w_{1i}} & \cdots & \frac{w_{Ii}}{w_{(i-1)i}} & \frac{w_{Ii}}{w_{(i+1)i}} & \cdots & 1 \end{bmatrix} \tag{13}$$

where w_{ij} denotes the final influence of the jth evaluation object on the ith evaluation object, and w_{ji} denotes that of the ith evaluation object on the jth evaluation object and $i \neq j$.

(3) The maximum eigenvectors $NCV_i = \begin{bmatrix} ncv_{i1} & ncv_{i2} & \cdots & ncv_{iI} \end{bmatrix}$ and $NEV_i = \begin{bmatrix} nev_{i1} \\ nev_{i2} \\ \vdots \\ nev_{iI} \end{bmatrix}$ of the causal and influence interaction comparison matrices for the ith evaluation object are,

respectively, calculated to form the reason matrix $NCM = \begin{bmatrix} ncv_{11} & ncv_{12} & \cdots & ncv_{1I} \\ ncv_{21} & ncv_{22} & \cdots & ncv_{2I} \\ \vdots & \vdots & \ddots & \vdots \\ ncv_{I1} & ncv_{I2} & \cdots & ncv_{II} \end{bmatrix}$ and the influence matrix $NEM = \begin{bmatrix} nev_{11} & nev_{21} & \cdots & nev_{I1} \\ nev_{12} & nev_{22} & \cdots & nev_{I2} \\ \vdots & \vdots & \ddots & \vdots \\ nev_{1I} & nev_{2I} & \cdots & nev_{II} \end{bmatrix}$. Based on this, the interaction strength matrix is calculated as

$$RNM = \begin{bmatrix} rnm_{11} & rnm_{12} & \cdots & rnm_{1I} \\ rnm_{21} & rnm_{22} & \cdots & rnm_{2I} \\ \vdots & \vdots & \ddots & \vdots \\ rnm_{I1} & rnm_{I2} & \cdots & rnm_{II} \end{bmatrix} \tag{14}$$

where $rnm_{ij} = \sqrt{ncv_{ij} \times nev_{ji}}$ and $0 \leq rnm_{ij} \leq 1$.

4. Bayesian FMEA

4.1. Bayesian Network

A Bayesian network can be represented by $BN = \langle \langle J, E \rangle L \rangle$ and consists of two parts:

(1) $\langle J, E \rangle$ is a directed acyclic graph composed of nodes and edges. Node J represents variables, and the directed edge E among nodes represents the relationships among variables [37]. The edge from node $J_{z\prime}(z\prime = 1, 2, \cdots, Z)$ to node $J_z(z = 1, 2, \cdots, Z)$ is represented by directed edge $E(J_{z\prime}, J_z)$. Here, $J_{z\prime}$ denotes the parent node of J_z, and J_z is the child node of $J_{z\prime}$ and $z\prime \neq z$. A node without a parent node is termed a root node, and one without a child node is termed a leaf node.

(2) L denotes the conditional probability distributions of nodes, reflecting the probability of a node's values, given its parent node states. In Bayesian networks with binary variables, a node with σ parent nodes requires 2^σ terms for its conditional probability table, which is difficult to determine when σ is large. The noisy-OR gate model, which only requires 2σ terms, was introduced to simplify this process [38]. It assumes the following: the input variables are independent and the output has a certain probability of being true when at least one input is true. Thus, the probability of the zth node J_z under all combinations of its parent node states can be obtained as

$$P(J_z|X(J_z)) = 1 - \prod_{z\prime=1}^{Z}(1 - \rho P(J_z|J_{z\prime})) \tag{15}$$

where $\rho = \begin{cases} 1, J_{z\prime} \in X(J_z) \\ 0, J_{z\prime} \notin X(J_z) \end{cases}$ and $X(J_z)$ denote all combinations of parent node states for the zth node J_z, and $P(J_z|J_{z\prime})$ denotes the probability of the zth node J_z occurring when the $z\prime$th node $J_{z\prime}$ occurs.

Given the prior probability distribution of the root nodes and the conditional probability distribution of the non-root nodes, the joint probability of all nodes in the Bayesian network [39] can be obtained as

$$P(J_1, J_2, \cdots, J_Z) = \prod_{z=1}^{Z} P(J_z|X(J_z)) \tag{16}$$

The $z\prime$th node $J_{z\prime}$ is then marginalized to obtain the joint probability of the other nodes as follows:

$$P(J_1, J_2, \cdots, J_{z\prime-1}, J_{z\prime+1}, \cdots, J_Z) = \sum_{J_{z\prime}} P(J_1, J_2, \cdots, J_Z) \tag{17}$$

Thus, the probability of the zth node J_z can be calculated using the total probability formula as

$$P(J_z) = \sum_{X(J_z)} P(J_z|X(J_z))P(X(J_z)) \tag{18}$$

where $P(X(J_z))$ denotes the joint probability of all parent–node state combinations for the zth node J_z.

4.2. Fault Mode Probability Calculation

This method utilizes GeNIe software (GeNIe Academic 4.1 version) to construct a Bayesian network for calculating the probability of each fault mode. The steps are:

(1) The severity and detection of fault modes are classified using Zhang's grading rule [40], and a Bayesian network is established based on the causal relationships among the fault modes, severity, detection, and risk factors.

(2) The interaction strengths from the hesitant fuzzy DSM are considered as conditional probabilities. Subsequently, the probability $P(R_n|R_{n'})$ of the nth risk factor $R_n(n = 1, 2, \cdots, N)$ given the n'th risk factor $R_{n'}(n' = 1, 2, \cdots, N)$, the probability $P(F_m|R_n)$ of the mth fault mode $F_m(m = 1, 2, \cdots, M)$ given the nth risk factor R_n, and the probability of the mth fault mode F_m given the m'th fault mode $F_{m'}(m' = 1, 2, \cdots, M)$ are obtained. $n' \neq n$ and $m' \neq m$.

(3) The probability $P(R_n)$ of the nth risk factor R_n, the joint probability $P(F_m, S_u)$ of the mth fault mode F_m and uth severity $S_u(u = 1, 2, \cdots, U)$, and the joint probability $P(F_m, D_v)$ of the mth fault mode F_m and vth detection $D_v(v = 1, 2, \cdots, V)$ are calculated using the fault data.

(4) The probabilities $P(R_n)$ of the nth risk factor R_n, $P(R_n|R_{n'})$ of the nth risk factor $R_n(n = 1, 2, \cdots, N)$ given the n'th risk factor $R_{n'}(n' = 1, 2, \cdots, N)$, $P(F_m|R_n)$ of the mth fault mode $F_m(m = 1, 2, \cdots, M)$ given the nth risk factor R_n, and $P(F_m|F_{m'})$ of the mth fault mode F_m given the m'th fault mode $F_{m'}(m' = 1, 2, \cdots, M)$ are input into the Bayesian network with $P(R_n)$ as the root node. Thus, the conditional probabilities of the nth risk factor R_n and mth fault mode F_m are calculated using Equation (15), and the probability $P(F_m)$ of the mth fault mode F_m is determined using Equations (16)–(18).

(5) The probabilities $P(S_u|F_m)$ that the mth fault mode F_m results in the uth severity S_u and $P(D_v|F_m)$ that the mth fault mode F_m has the vth detection D_v are calculated using Equations (16) and (17), incorporating the joint probabilities $P(F_m, S_u)$ of the mth fault mode F_m and uth severity level S_u and $P(F_m, D_v)$ of the mth fault mode F_m and vth detection level D_v, and the probability of $P(F_m)$ of the mth fault mode F_m.

(6) The probabilities $P(S_u|F_m)$ that the mth fault mode F_m results in the uth severity S_u and the $P(D_v|F_m)$ that the mth fault mode F_m has the vth detection D_v are input to the Bayesian network. The conditional probabilities of the uth severity S_u and vth detection D_v are then calculated using Equation (15) to develop a complete Bayesian network probability model.

(7) In the Bayesian network probability model, updating the network can yield the probability $P(F_m|S_u, D_v)$ of the mth fault mode F_m at the uth severity S_u and the vth detection D_v when the probabilities $P(S_u)$ of a fault consequence at the uth severity S_u and the $P(D_v)$ of fault detection at the vth detection D_v are both 100%.

4.3. Fault Risk Assessment

Based on the probability $P(F_m|S_u, D_v)$ of the mth fault mode F_m at the uth severity S_u and vth detection D_v and the severity and detection scores in Table 3, the RPN of the mth fault mode F_m is calculated as follows:

$$RPN_m = P(F_m|S_u, D_v) \times S(u) \times D(v) \tag{19}$$

where $S(u)$ denotes the severity score of the uth level, and $D(v)$ denotes the detection score of the vth level, and $0 \leq RPN_m \leq 49$.

Table 3. Severity and detection of fault modes.

Level	Severity Number	Level Definition	Detection Number	Level Definition	Score
1	S1	The influence is minimal, with no significant effect on system operation or security	D1	Detection is simple through routine checks or monitoring systems	1
2	S2	The system remains unaffected and needs only minor adjustments	D2	Easily detectable but needs specific testing methods	2
3	S3	The system's operational efficiency slightly decreases, allowing for quick repairs	D3	Moderately detectable, requiring professional tools for inspection or analysis	3
4	S4	The issue partially affects a single device, which can be restored with backups or simple repairs, and has minimal impact on the overall system	D4	Detection is difficult and requires complex testing or advanced analysis	4
5	S5	The issue leads to a partial system shutdown, causing longer maintenance and moderate effects on production plans	D5	Detection is challenging and requires expertise and specialized equipment	5
6	S6	The malfunction of critical equipment components has restricted system operations, adversely affecting production goals	D6	Detection is rather challenging and requires advanced technology	6
7	S7	The malfunction of critical equipment has caused system failures and extended repair times, greatly affecting production	D7	Detection and prediction are nearly impossible until serious consequences occur	7

5. Critical Fault Identification and Maintenance Decision-Making Method

5.1. Critical Fault Identification

The hesitant fuzzy DSM and Bayesian FMEA are employed to identify the critical fault modes in a stacker-automated stereoscopic warehouse, as shown in Figure 1. The steps are as follows:

(1) Fault modes, risk factors, and consequences are summarized based on fault data from the stacker-automated stereoscopic warehouse. Subsequently, the severity and detection of the fault modes are classified using Table 3.

(2) A hesitant fuzzy evaluation of the influence among risk factors and fault modes in the stacker-automated stereoscopic warehouse is performed using Table 4, and the final expert weights are calculated using Equations (1)–(8). Subsequently, in combination with the final expert weights and evaluation sets, the final influence among risk factors and fault modes is calculated using Equations (9)–(11).

(3) A risk structure matrix for risk factors and fault modes is established based on the final influence among risk factors and fault modes in the stacker-automated stereoscopic warehouse. The matrix is decomposed and transformed using Equations (12)–(14) to obtain the interaction strength matrix among risk factors and fault modes.

(4) A Bayesian network is established to show the causal relationships among fault modes, severity, detection, and risk factors in the stacker-automated stereoscopic warehouse, and then the fault risk levels of fault modes are evaluated using Equations (15)–(19).

(5) The fault modes of the stacker-automated stereoscopic warehouse are sorted according to their RPNs, and the top 20% are selected as critical fault modes using Rakyta's method [41].

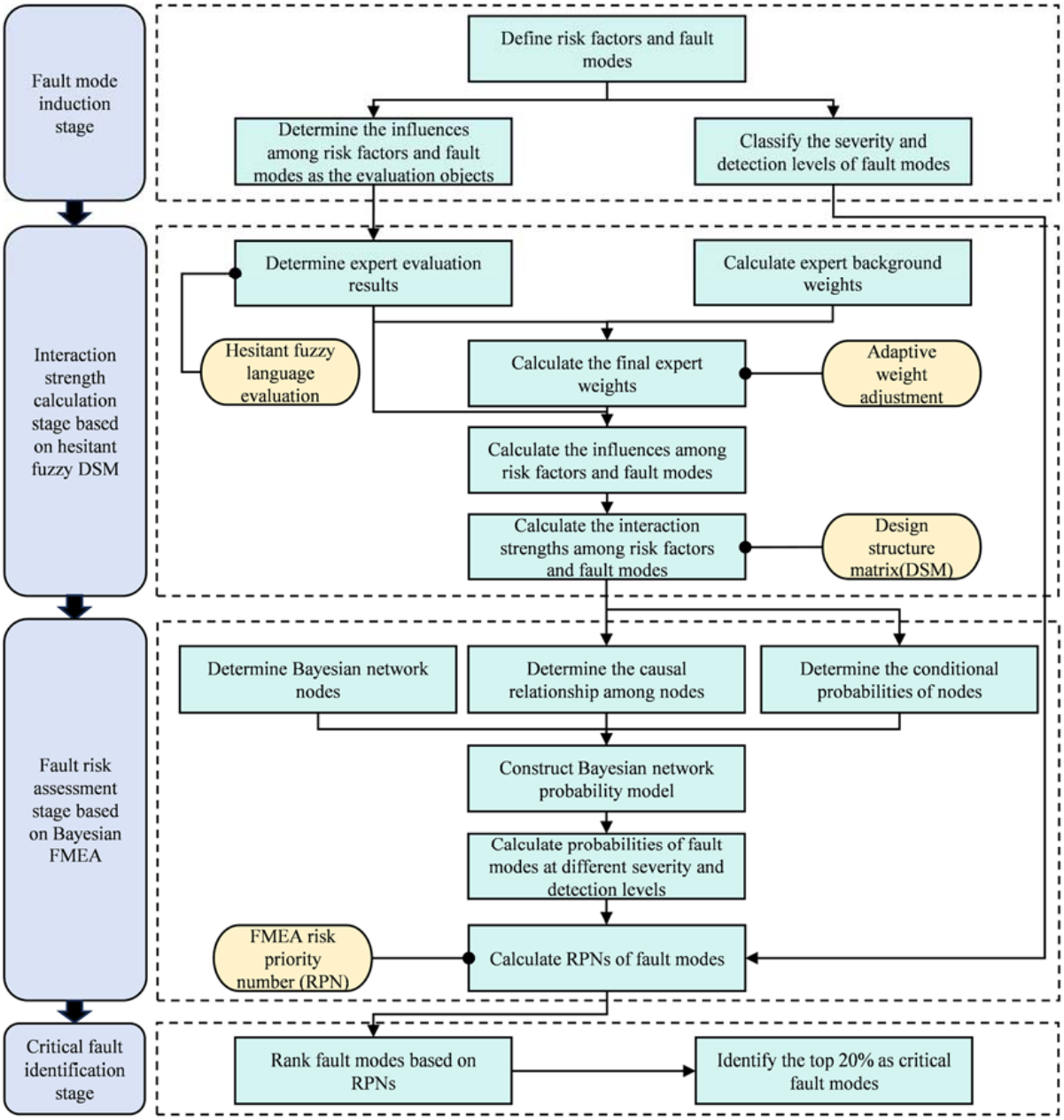

Figure 1. Critical fault identification process for stacker-automated stereoscopic warehouses.

Table 4. Fuzzy language evaluation set for influence.

Level	Relationship Representation	Trapezoidal Fuzzy Number	Language Evaluation
0	N	(0, 0, 0, 0)	No influence
1	L	(0, 1, 1, 2)	Low influence
2	BLM	(2, 3, 3, 4)	Between low and moderate influence
3	M	(4, 5, 5, 6)	Moderate influence
4	BMH	(6, 7, 7, 8)	Between moderate and high influence
5	H	(8, 8, 9, 9)	High influence
6	VH	(9, 9, 10, 10)	Very high influence

5.2. Formulation of Maintenance Strategies for Fault Modes

Fault maintenance is vital for the operation of stacker-automated stereoscopic warehouses and focuses on minimizing faults through preventive measures and timely responses [42]. Researchers examined various fault-maintenance strategies. Liu et al. [43] classified six maintenance strategies based on their effectiveness: better-than-perfect, perfect, imperfect, minimal, worse-than-minimal, and worst. Li et al. [44] categorized strategies as corrective, time-based, condition-based, and predictive maintenance. Bram et al. [45] categorized them into corrective and preventive maintenance, with preventive maintenance further subdivided into time-, age-, and usage-based maintenance. Cheikh et al. [46] also classified strategies as corrective and preventive maintenance, where corrective maintenance refers to breakdown maintenance and preventive maintenance is further divided into condition-based and periodic maintenance. Aafif et al. [47] classified strategies as regular- and alternating-use maintenance. Stacker-automated stereoscopic warehouses require maintenance strategies that can quickly address and prevent faults. However, Liu et al. [43], Li et al. [44], and Bram et al. [45] proposed overly detailed strategies that incurred high costs and practical challenges, whereas Aafif et al. [47] offered an overly simple approach with ineffective fault prevention. In contrast, Cheikh et al. [46] proposed balanced strategies. Therefore, maintenance strategies are categorized as condition-based, periodic, or breakdown maintenance, as described by Cheikh et al. [46]. For high-risk fault modes, condition-based maintenance allows for the timely detection of issues, prevention of major losses, and enhancement of system reliability. Although initial investment is high, it can lead to significant long-term savings by extending equipment lifespan and reducing unplanned downtime. Periodic maintenance can prevent faults in moderate-risk fault modes and is more cost-effective than condition-based maintenance [48]. Low-risk fault modes typically have minimal impact, and thus breakdown maintenance is used to reduce costs and focus resources on critical issues [49]. Thus, maintenance strategies of fault modes are determined using the method proposed by Mohd et al. [50] based on risk assessment results.

Based on the RPNs of fault modes, three-level boundary values are calculated as

$$\begin{cases} G_1 = b + \frac{c-b}{3} \\ G_2 = b + 2 \times \frac{c-b}{3} \end{cases} \tag{20}$$

where c denotes the maximum RPN, and b is the minimum. The maintenance decision-making rules for fault modes in the stacker-automated stereoscopic warehouse are outlined in Table 5 using the three-level boundary values, i.e., G_1 and G_2, with the characteristics of each maintenance strategy.

Table 5. Maintenance decision-making rules for fault modes.

Maintenance Strategy	Fault Risk Level
Condition-based maintenance	$(G_2, c]$
Periodic maintenance	$(G_1, G_2]$
Breakdown maintenance	$[b, G_1]$

6. Case Study

Company A manufactures and sells household appliances and engages in import and export activities. Its stacker-automated stereoscopic warehouse covers 1718 m^2, facilitating transportation, storage, picking, and delivery of products. The warehouse features the following five areas: vertical storage, second-floor storage, second-floor flipping storage, first-floor outbound shipping, and first-floor transfer storage. As shown in Figure 2, the

hardware components include a shelving system, stacker system, and transportation system with the specific parameters listed in Table 6.

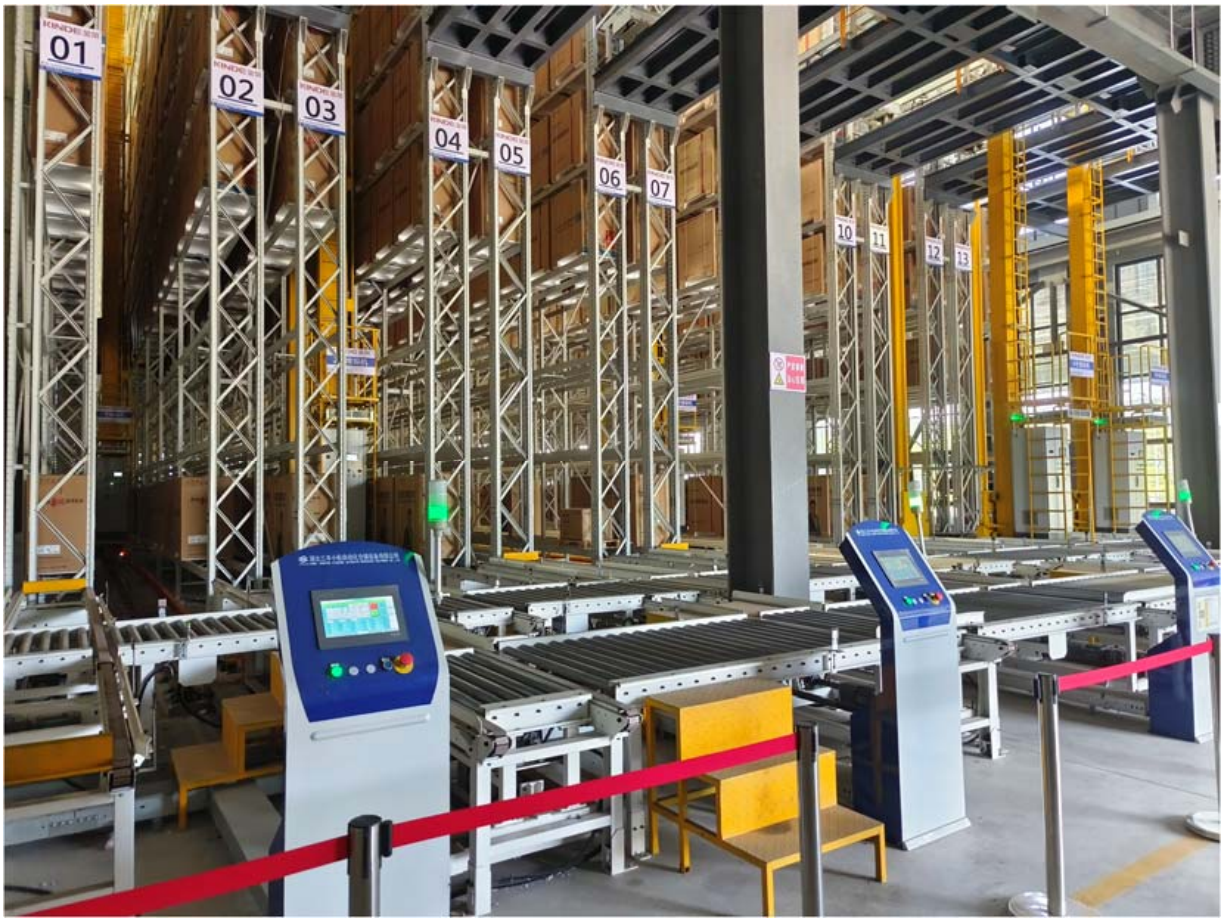

Figure 2. Stacker-automated stereoscopic warehouse in Company A.

6.1. Hesitant Fuzzy Evaluation of the Influence

First, 34 fault modes and 12 risk factors are identified from Company A's stacker-automated stereoscopic warehouse data, as summarized in Tables 7 and 8. The severity and detection of these fault modes are listed in Table 3. Second, an FMEA team of five experts is formed, and their backgrounds are detailed in Table 9. The background weights are calculated using Equation (1) and Table 2, as listed in Table 9. Third, a hesitant fuzzy evaluation is conducted using Table 4 on the influences of 34 fault modes and 12 risk factors, revealing five pairs of interactive risk factors, 57 pairs of interactive fault modes, and 164 pairs of interactive fault modes and risk factors. Table 10 present the expert evaluation sets for the influences. Fourth, when combined with the expert evaluation set of the influences among the 34 fault modes and 12 risk factors and the expert background weights in Table 9, the final expert weights are calculated using Equations (2)–(8), as listed in Table 11. The final influence is calculated using Equations (9)–(11).

Table 6. Partial parameters of stacker-automated stereoscopic warehouse in Company A.

Equipment Name		Brand Selection	Equipment Name		Brand Selection
Rack system	Rack	Main material Q355B, other materials Q235B, 14 × 14	Stacker system	Shuttle	MIAS/LHD/Apes Fork
	Storage location	1130 mm × 670 mm × 1200 mm		Wire rope	German Pfeifer
Stacker system	Stacker	Double-extension double-mast single-station stacker		VFD	Siemens/Schneider
	Ground rail	30 kg	Transportation system	Motor	SEW/NORD
	Ceiling rail	100 mm × 100 mm × 10 mm Angle steel		VFD	Siemens /Danfoss
	Sliding rail	Panasonic /Vahle		Detection device	OMRON
	Travelling addressing system	German Sick/Leuze		Low-voltage apparatus	Schneider
	Lifting addressing system	German Sick		Conveyor chain	Hangzhou Donghua /Anhui Huangshan
	Critical position bearing	Swedish SKF/NSK		Drive chain	Hangzhou Donghua/Anhui Huangshan
	Travelling wheel	Komatsu		Bearing part	Dongguan Bearing factory/Haerbin Bearing factory, TR/SKF
	Motor	SEW		Lamp	Schneider/APT

Table 7. Fault modes of Company A's stacker-automated stereoscopic warehouse.

Number	Fault Mode	Number	Fault Mode
F1	Noise	F18	Break of wire rope of the stacker lifting mechanism
F2	Mechanical wear of ground rail	F19	Abnormal pulling marks on the guiding rail of the stacker lifting mechanism
F3	Addressing fault of stacker shuttle	F20	Stacker motor overheating
F4	Shaking of stacker frame beam	F21	Stacker shuttle exceeds the limit
F5	Fault of laser rangefinder of stacker horizontal travelling mechanism	F22	Stacker shuttle shaking
F6	Cracks in the weld seam of stacker mast	F23	Stacker shuttle timeout
F7	Damage of travelling wheels of stacker horizontal travelling mechanism	F24	Stacker shuttle does not extend smoothly
F8	Stuck of stacker guiding wheels	F25	Break of conveyor chain of transportation system
F9	Clearance or separation of stacker guiding wheels	F26	Stuck or leaking of conveyor chain of transportation system
F10	Damage of stacker reducer	F27	Unstable conveyor belt of transportation system

Table 7. *Cont.*

Number	Fault Mode	Number	Fault Mode
F11	Damage of stacker VDF	F28	Fault of forklift operation of transportation system
F12	Damage of stacker brake	F29	Damage of rack
F13	Tripping of stacker control switch	F30	Settlement of rack
F14	Damage of stacker limiting switch	F31	Empty pickup and empty outbound
F15	Position deviation of stacker horizontal travelling mechanism	F32	Double storage and double unloading
F16	Damage of rope winding device of stacker lifting mechanism	F33	Fault of scanning device
F17	Damage of stacker lifting mechanism	F34	The stacking type of goods in the rack is not standardized

Table 8. Risk factors of Company A's stacker-automated stereoscopic warehouse.

Number	Risk Factor	Number	Risk Factor
R1	Is the material qualified?	R7	Is the maintenance strategy reasonable?
R2	Is the quality of the parts qualified?	R8	Work overload
R3	Is the quality of the assembly qualified?	R9	Variable workload
R4	Equipment aging or long service life	R10	Improper operation by workers
R5	Equipment damage	R11	Is the operating environment suitable?
R6	Is the equipment regularly maintained?	R12	Is the information system functioning properly?

Table 9. Backgrounds and weights of five experts.

Number	Position	Educational Level	Work Experience	Age	Familiarity Level	Score	Background Weights
1	General operators	Undergraduate	1–5 years	20–25	Familiar	9	0.117
2	Technician	Master	1–5 years	25–30	Between understanding and familiar	11	0.143
3	Junior researcher	Master	6–10 years	25–30	Familiar	14	0.182
4	Senior researcher	Doctor	11–20 years	31–40	Very familiar	20	0.26
5	Senior expert	Doctor	20–30 years	50–60	Between familiar and very familiar	23	0.299

Table 10. Five expert evaluation sets for the influence among interacting risk factors.

Number	Risk Factor	Expert Evaluation Level				
		1	**2**	**3**	**4**	**5**
1	R1→R2	6	5	4	4, 5	4, 5
2	R2→R3	4, 5	4	5	3, 4	4
3	R6→R4	5	5	5, 6	4	5
4	R11→R4	3	2, 3	3	3, 4	4
5	R8→R5	4	3, 4	3	3	3

Table 11. Final weights of five experts.

Expert Number	Final Weights of Experts		
	When Evaluating the Interactions Among Risk Factors	**When Evaluating the Interactions Among Risk Factors and Fault Modes**	**When Evaluating the Interactions Among Fault Modes**
1	0.081	0.101	0.092
2	0.131	0.120	0.136
3	0.147	0.163	0.155
4	0.258	0.248	0.244
5	0.384	0.368	0.374

6.2. Interaction Strength Calculation

The risk structure matrix L_1 is established based on the final influence among 34 fault modes and 12 risk factors. Then, the risk structure matrix L_1 is decomposed and transformed using Equations (12)–(14) to obtain the interaction strength matrix L_2.

$$L_1 = \begin{bmatrix} 0 & 0 & 0 & 0 & 0 & 0 & 0 & 0 & 0 & 0 & 0 & 0 & 0 & \cdots & 0 \\ 0.762 & 0 & 0 & 0 & 0 & 0 & 0 & 0 & 0 & 0 & 0 & 0 & 0 & \cdots & 0 \\ 0 & 0.685 & 0 & 0 & 0 & 0 & 0 & 0 & 0 & 0 & 0 & 0 & 0 & \cdots & 0 \\ 0 & 0 & 0 & 0 & 0 & 0.790 & 0 & 0 & 0 & 0 & 0.682 & 0 & 0 & \cdots & 0 \\ 0 & 0 & 0 & 0 & 0 & 0 & 0 & 0.527 & 0 & 0 & 0 & 0 & 0 & \cdots & 0 \\ \vdots & \vdots & \vdots & \vdots & \vdots & \vdots & \vdots & \vdots & \vdots & \vdots & \vdots & \vdots & \vdots & \ddots & \vdots \\ 0 & 0 & 0.751 & 0.471 & 0 & 0.619 & 0.682 & 0.476 & 0.485 & 0.447 & 0.550 & 0 & 0 & \cdots & 0 \\ 0.571 & 0.561 & 0.743 & 0 & 0 & 0.541 & 0.696 & 0.757 & 0.816 & 0.701 & 0.517 & 0 & 0 & \cdots & 0 \\ 0 & 0 & 0 & 0 & 0 & 0 & 0 & 0 & 0.314 & 0.800 & 0 & 0.804 & 0 & \cdots & 0.745 \\ 0 & 0 & 0.785 & 0 & 0 & 0.392 & 0 & 0.296 & 0.496 & 0 & 0.373 & 0 & 0 & \cdots & 0 \\ 0 & 0 & 0 & 0.850 & 0 & 0.844 & 0.489 & 0 & 0 & 0 & 0 & 0 & 0 & \cdots & 0 \\ 0.838 & 0 & 0 & 0.587 & 0 & 0.555 & 0 & 0 & 0 & 0 & 0.313 & 0 & 0 & \cdots & 0 \\ 0.743 & 0.493 & 0.640 & 0 & 0 & 0.706 & 0.471 & 0.662 & 0.463 & 0 & 0.463 & 0 & 0 & \cdots & 0 \\ \vdots & \vdots & \vdots & \vdots & \vdots & \vdots & \vdots & \vdots & \vdots & \vdots & \vdots & \vdots & \vdots & \ddots & \vdots \\ 0 & 0 & 0 & 0 & 0 & 0 & 0 & 0 & 0.804 & 0 & 0.657 & 0 & 0.444 & 0 & 0 \end{bmatrix}$$

$$L_2 = \begin{bmatrix} 0 & 0 & 0 & 0 & 0 & 0 & 0 & 0 & 0 & 0 & 0 & 0 & 0 & \cdots & 0 \\ 0.623 & 0 & 0 & 0 & 0 & 0 & 0 & 0 & 0 & 0 & 0 & 0 & 0 & \cdots & 0 \\ 0 & 0.587 & 0 & 0 & 0 & 0 & 0 & 0 & 0 & 0 & 0 & 0 & 0 & \cdots & 0 \\ 0 & 0 & 0 & 0 & 0 & 0.462 & 0 & 0 & 0 & 0 & 0.437 & 0 & 0 & \cdots & 0 \\ 0 & 0 & 0 & 0 & 0 & 0 & 0 & 0.497 & 0 & 0 & 0 & 0 & 0 & \cdots & 0 \\ \vdots & \vdots & \vdots & \vdots & \vdots & \vdots & \vdots & \vdots & \vdots & \vdots & \vdots & \vdots & \vdots & \ddots & \vdots \\ 0 & 0 & 0.364 & 0.211 & 0 & 0.254 & 0.338 & 0.235 & 0.256 & 0.246 & 0.318 & 0 & 0 & \cdots & 0 \\ 0.288 & 0.278 & 0.358 & 0 & 0 & 0.226 & 0.342 & 0.378 & 0.428 & 0.319 & 0.281 & 0 & 0 & \cdots & 0 \\ 0 & 0 & 0 & 0 & 0 & 0 & 0 & 0 & 0.174 & 0.385 & 0 & 0.482 & 0 & \cdots & 0.647 \\ 0 & 0 & 0.457 & 0 & 0 & 0.193 & 0 & 0.175 & 0.315 & 0 & 0.246 & 0 & 0 & \cdots & 0 \\ 0 & 0 & 0 & 0.470 & 0 & 0.427 & 0.298 & 0 & 0 & 0 & 0 & 0 & 0 & \cdots & 0 \\ 0.542 & 0 & 0 & 0.336 & 0 & 0.299 & 0 & 0 & 0 & 0 & 0.219 & 0 & 0 & \cdots & 0 \\ 0.376 & 0.246 & 0.320 & 0 & 0 & 0.290 & 0.233 & 0.326 & 0.244 & 0 & 0.254 & 0 & 0 & \cdots & 0 \\ \vdots & \vdots & \vdots & \vdots & \vdots & \vdots & \vdots & \vdots & \vdots & \vdots & \vdots & \vdots & \vdots & \ddots & \vdots \\ 0 & 0 & 0 & 0 & 0 & 0 & 0 & 0 & 0.482 & 0 & 0.365 & 0 & 0.374 & 0 & 0 \end{bmatrix}$$

6.3. Probability Calculation of Fault Modes

Initially, a Bayesian network is developed based on the interactions of 34 fault modes and 12 risk factors (see Figure 3) to analyze fault modes, risk factors, severity, and detection of the stacker-automated stereoscopic warehouse in Company A. Second, conditional probabilities for the 12 risk factors and 34 fault modes are calculated using the probabilities derived from the interaction intensity matrix and Equation (15). Subsequently, the probabilities of the 34 fault modes are determined using Equations (16)–(18). By combining the probabilities of the 34 fault modes with their joint probabilities concerning severity and detection, probabilities of their severity and detection belonging to different severities and detection levels are calculated using Equations (16)–(17). The conditional probability tables for varying severity and detection are established using Equation (15), and a Bayesian network probability model is established as shown in Figure 4. Finally, by setting the probabilities of each severity and detection level to 100%, the probabilities of the fault modes at different severities and detection levels are obtained by updating the network, as listed in Table 12.

Table 12. Probability P(F/S, D) of each fault mode F at each severity S and detection D.

P (F/S, D)	Value	P (F/S, D)	Value	P(F/S, D)	Value
P (F1/S1, D4)	0.95	P (F12/S6, D2)	0.861	P (F22/S2, D2)	0.41
P (F1/S1, D3)	0.941	P (F12/S6, D4)	0.868	P (F23/S3, D1)	0.698
P (F2/S2, D3)	0.835	P (F13/S4, D4)	0.811	P (F24/S3, D2)	0.635
P (F2/S2, D1)	0.834	P (F13/S4, D2)	0.788	P (F25/S4, D2)	0.824
P (F3/S3, D5)	0.934	P (F14/S6, D5)	0.724	P (F26/S4, D2)	0.687
P (F4/S4, D2)	0.822	P (F14/S6, D2)	0.709	P (F27/S4, D4)	0.795
P (F4/S4, D3)	0.822	P (F15/S2, D4)	0.899	P (F28/S3, D5)	0.755
P (F5/S3, D3)	0.511	P (F15/S2, D3)	0.888	P (F29/S2, D1)	0.839
P (F6/S7, D7)	1	P (F16/S1, D3)	0.887	P (F30/S2, D1)	0.374
P (F7/S2, D2)	0.945	P (F17/S4, D5)	0.818	P (F31/S2, D1)	0.447
P (F7/S2, D1)	0.943	P (F17/S4, D6)	0.922	P (F31/S2, D2)	0.445
P (F7/S2, D5)	0.947	P (F18/S4, D1)	0.902	P (F32/S2, D1)	0.432
P (F8/S4, D4)	0.631	P (F19/S2, D3)	0.897	P (F32/S2, D2)	0.43
P (F8/S4, D6)	0.707	P (F20/S5, D4)	0.909	P (F33/S1, D1)	0.544
P (F9/S5, D2)	0.862	P (F20/S5, D3)	0.902	P (F33/S1, D3)	0.542
P (F10/S2, D3)	0.645	P (F21/S2, D2)	0.757	P (F34/S3, D1)	0.846
P (F11/S3, D4)	0.674	P (F21/S2, D5)	0.785	P (F34/S3, D3)	0.844

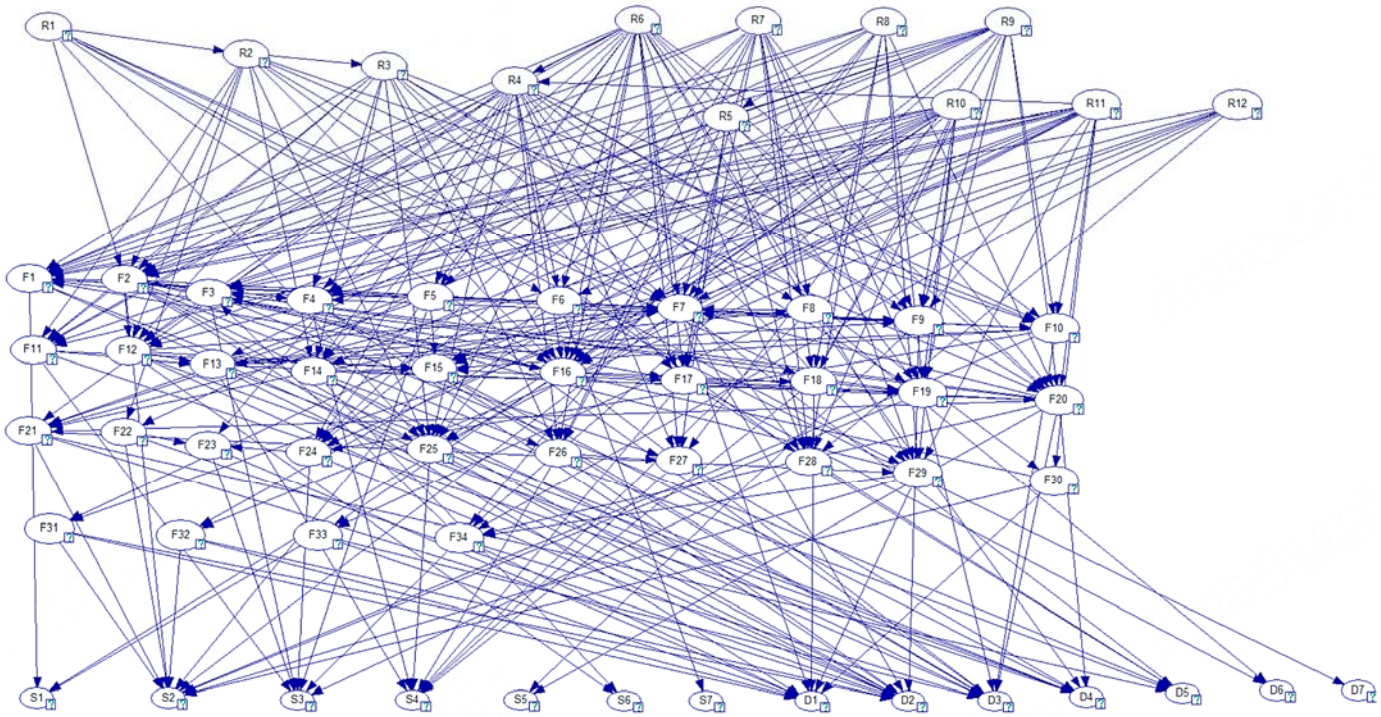

Figure 3. Bayesian network of Company A's stacker-automated stereoscopic warehouse.

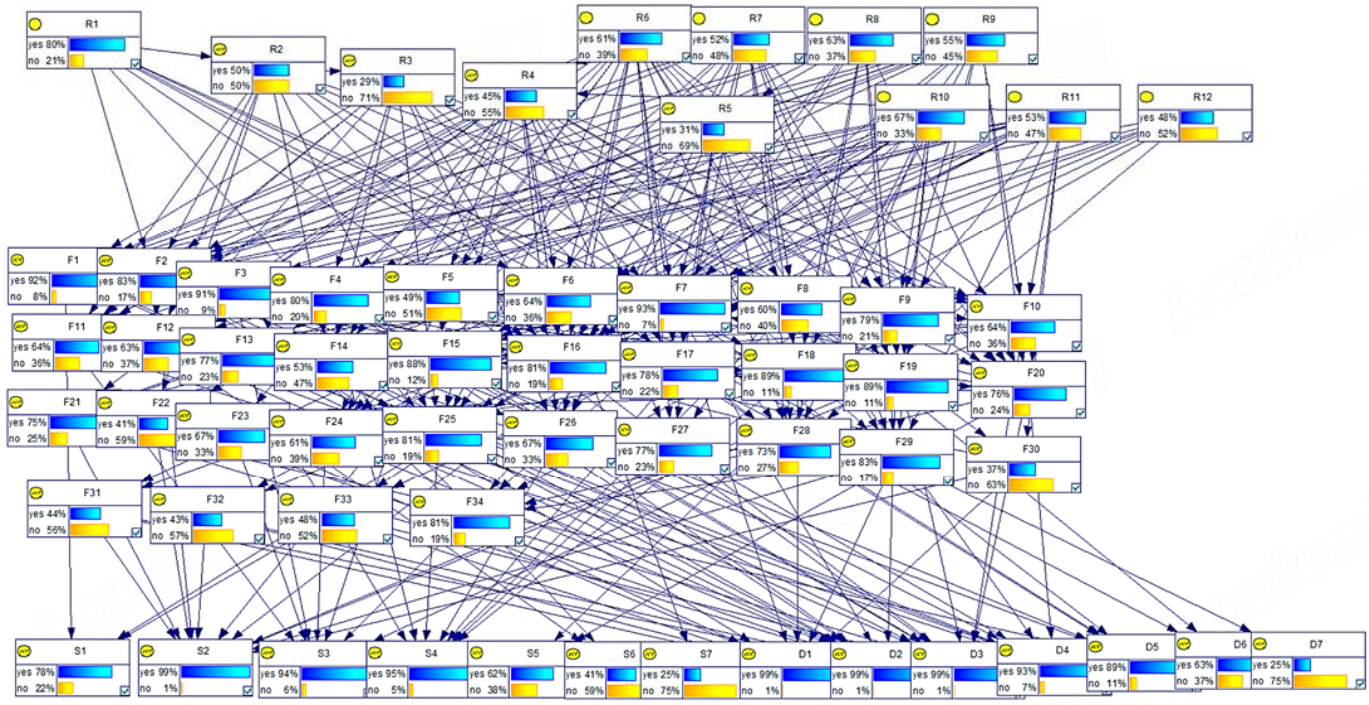

Figure 4. Bayesian network probability model of Company A's stacker-automated stereoscopic warehouse.

6.4. Critical Fault Identification and Maintenance Decision-Making

First, the RPN of each fault mode is calculated using Equation (19), which considers the probabilities of the fault modes at different severities and detection levels from Table 12 and the scores from Table 3. The 34 fault modes of the stacker-automated stereoscopic warehouse are ranked in Table 13, with the top 20% identified as critical fault modes for Company A's stacker-automated stereoscopic warehouse: F6, F17, F20, F12, F14, and F8.

As shown in Table 13, the highest RPN corresponds to F6, whereas the lowest is for F30. Finally, the three-level boundary values $G_1 = 16.823$ and $G_2 = 32.916$ are calculated using Equation (20), and the highest RPN, lowest RPN, and maintenance strategies for the 34 fault modes are determined using Table 5 and shown in Table 14.

Table 13. RPNs of fault modes.

Fault Mode	Probability		Severity	Detection	RPN	Total RPN	Ranking
F1	P (F1/S1, D4)	0.95	1	4	3.8	6.623	19
	P (F1/S1, D3)	0.941	1	3	2.823		
F2	P (F2/S2, D3)	0.835	2	3	5.01	6.678	18
	P (F2/S2, D1)	0.834	2	1	1.668		
F3	P (F3/S3, D5)	0.934	3	5	14.01	14.01	10
F4	P (F4/S4, D2)	0.822	4	2	6.576	16.44	8
	P (F4/S4, D3)	0.822	4	3	9.864		
F5	P (F5/S3, D3)	0.511	3	3	4.599	4.599	23
F6	P (F6/S7, D7)	1	7	7	49	49	1
F7	P (F7/S2, D2)	0.945	2	2	3.78	15.136	9
	P (F7/S2, D1)	0.943	2	1	1.886		
	P (F7/S2, D5)	0.947	2	5	9.47		
F8	P (F8/S4, D4)	0.631	4	4	10.096	27.064	6
	P (F8/S4, D6)	0.707	4	6	16.968		
F9	P (F9/S5, D2)	0.862	5	2	8.62	8.62	16
F10	P (F10/S2, D3)	0.645	2	3	3.87	3.87	24
F11	P (F11/S3, D4)	0.674	3	4	8.088	8.088	17
F12	P (F12/S6, D2)	0.861	6	2	10.332	31.164	4
	P (F12/S6, D4)	0.868	6	4	20.832		
F13	P (F13/S4, D4)	0.811	4	4	12.976	19.28	7
	P (F13/S4, D2)	0.788	4	2	6.304		
F14	P (F14/S6, D5)	0.724	6	5	21.72	30.228	5
	P (F14/S6, D2)	0.709	6	2	8.508		
F15	P (F15/S2, D4)	0.899	2	4	7.192	12.52	12
	P (F15/S2, D3)	0.888	2	3	5.328		
F16	P (F16/S1, D3)	0.887	1	3	2.661	2.661	28
F17	P (F17/S4, D5)	0.818	4	5	16.36	38.488	2
	P (F17/S4, D6)	0.922	4	6	22.128		
F18	P (F18/S4, D1)	0.902	4	1	3.608	3.608	26
F19	P (F19/S2, D3)	0.897	2	3	5.382	5.382	22
F20	P (F20/S5, D4)	0.909	5	4	18.18	31.71	3
	P (F20/S5, D3)	0.902	5	3	13.53		
F21	P (F21/S2, D2)	0.757	2	2	3.028	10.878	14
	P (F21/S2, D5)	0.785	2	5	7.85		
F22	P (F22/S2, D2)	0.41	2	2	1.64	1.64	33
F23	P (F23/S3, D1)	0.698	3	1	2.094	2.094	31
F24	P (F24/S3, D2)	0.635	3	2	3.81	3.81	25
F25	P (F25/S4, D2)	0.824	4	2	6.592	6.592	20
F26	P (F26/S4, D2)	0.687	4	2	5.496	5.496	21
F27	P (F27/S4, D4)	0.795	4	4	12.72	12.72	11
F28	P (F28/S3, D5)	0.755	3	5	11.325	11.325	13
F29	P (F29/S2, D1)	0.839	2	1	1.678	1.678	32
F30	P (F30/S2, D1)	0.374	2	1	0.748	0.748	34
F31	P (F31/S2, D1)	0.447	2	1	0.894	2.674	27
	P (F31/S2, D2)	0.445	2	2	1.78		
F32	P (F32/S2, D1)	0.432	2	1	0.864	2.584	29
	P (F32/S2, D2)	0.43	2	2	1.72		

Table 13. *Cont.*

Fault Mode	Probability		Severity	Detection	RPN	Total RPN	Ranking
F33	P (F33/S1, D1)	0.544	1	1	0.544	2.17	30
	P (F33/S1, D3)	0.542	1	3	1.626		
F34	P (F34/S3, D1)	0.846	3	1	2.538	10.134	15
	P (F34/S3, D3)	0.844	3	3	7.596		

Table 14. Maintenance strategies for fault modes.

Maintenance Strategy	RPN	Fault Modes
Condition-based maintenance	(32.916, 49]	F6, F17
Periodic maintenance	(16.832, 32.916]	F8, F12, F13, F14, F20
Breakdown maintenance	[0.748, 16.832]	F1, F2, F3, F4, F5, F7, F9, F10, F11, F15, F16, F18, F19, F21, F22, F23, F24, F25, F26, F27, F28, F29, F30, F31, F32, F33, F34

6.5. Results and Analysis

Figure 5 presents a radar chart illustrating the Risk Priority Numbers (RPNs) of the six critical fault modes. As known from Figure 5, F6 is the most critical fault mode, with the potential to cause equipment tilting or collapse, resulting in significant machinery damage and safety risks for operators. This can lead to production interruptions and increased maintenance costs. F17 is the second most critical fault mode, hindering the stacker's ability to lift and unload goods effectively, severely impacting warehouse operations. A malfunction at high elevations may cause goods to fall, damaging products and creating safety hazards. F20 and F12 have comparable RPN values and are classified as high-risk fault modes. F20 can cause motor overheating, potentially disabling the stacker and igniting a fire, posing a significant threat to warehouse equipment and stored goods. Similarly, F12 may result in inaccurate stopping of the stacker, leading to collisions and damage to goods or equipment, and in severe cases, loss of control, creating serious safety hazards. F14 and F8 also present high fault risks. F14 may cause the stacker to exceed safe operating limits, resulting in collisions or equipment damage, and may impair the stacker's ability to accurately locate goods, leading to operational errors and decreased efficiency. F8 can cause stacker malfunctions, significantly affecting warehouse operational efficiency. If these faults are not promptly addressed, they may worsen the wear and tear on other components, further increasing the risk of equipment failure. These fault modes are critical for stacker-automated stereoscopic warehouses due to their high RPN values and significant impact on system safety and operational efficiency. Therefore, Company A should prioritize addressing them.

Table 15 outlines the critical fault modes for Company A's stacker-automated stereoscopic warehouse and their corresponding maintenance strategies. Company A identified critical fault modes and maintenance strategies for its stacker-automated stereoscopic warehouse based on expert experience and the manufacturer's manual. The critical fault modes are F17, F20, F12, and F14, which primarily use breakdown maintenance with periodic maintenance as a supplement. However, the proposed method identified additional fault modes: F6, F17, F20, F12, F14, and F8. F6 and F17 used condition-based maintenance, whereas the others relied on periodic maintenance. This method uncovered more critical fault modes, particularly F6 and F8, which are typically overlooked by traditional approaches and are susceptible to various risk factors and other fault modes. Moreover, in contrast to Company A's existing strategy, the proposed method provides more targeted

and objective maintenance strategies that vary with fault risks, receiving unanimous recognition from the management and maintenance personnel. The results demonstrated the effectiveness and superiority of the proposed method.

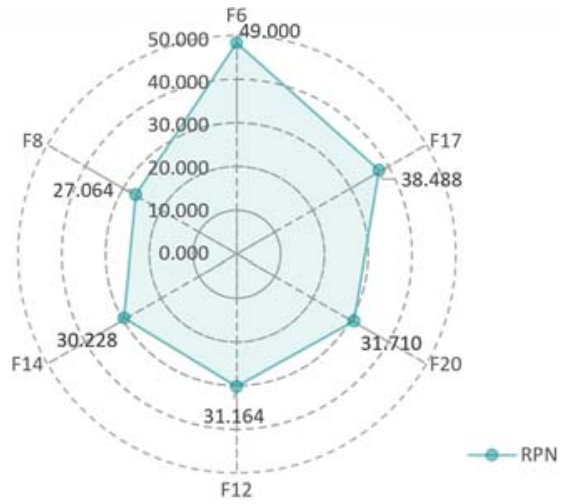

Figure 5. RPN radar chart for six critical fault modes.

Table 15. Six critical fault modes and their maintenance strategies.

Fault Mode	Description	RPN	Maintenance Strategy
F6	Cracks in the weld seam of stacker mast	49.000	Condition-based maintenance
F17	Damage of stacker lifting mechanism	38.488	Condition-based maintenance
F20	Stacker motor overheating	31.710	Periodic maintenance
F12	Damage of stacker brake	31.164	Periodic maintenance
F14	Damage of stacker limiting switch	30.228	Periodic maintenance
F8	Stuck of stacker guiding wheels	27.064	Periodic maintenance

The proposed Bayesian FMEA was compared with the traditional FMEA [51], fuzzy FMEA [52], and fuzzy FMEA considering multiple risk factors [3] to validate its effectiveness and superiority. The results are summarized in Table 16 and Figure 6, and analyzed as follows:

Table 16. RPN rankings of different FMEAs.

Fault Mode	Bayesian FMEA	Traditional FMEA	Fuzzy FMEA	Fuzzy FMEA Considering Multiple Risk Factors	Fault Mode	Bayesian FMEA	Traditional FMEA	Fuzzy FMEA	Fuzzy FMEA Considering Multiple Risk Factors
F1	19	29	31	28	F18	26	25	32	29
F2	18	16	16	14	F19	22	27	20	20
F3	10	5	7	7	F20	3	4	1	1
F4	8	12	13	5	F21	14	9	10	11
F5	23	15	17	10	F22	33	28	30	31
F6	1	3	3	4	F23	31	24	26	25
F7	9	7	4	8	F24	25	20	23	24
F8	6	6	8	3	F25	20	21	21	21
F9	16	14	19	18	F26	21	17	24	22
F10	24	22	22	23	F27	11	11	9	12
F11	17	19	12	13	F28	13	17	15	16
F12	4	2	2	2	F29	32	33	34	27
F13	7	8	11	15	F30	34	31	27	32
F14	5	1	5	9	F31	27	30	28	33

Table 16. *Cont.*

Fault Mode	Bayesian FMEA	Traditional FMEA	Fuzzy FMEA	Fuzzy FMEA Considering Multiple Risk Factors	Fault Mode	Bayesian FMEA	Traditional FMEA	Fuzzy FMEA	Fuzzy FMEA Considering Multiple Risk Factors
F15	12	26	18	26	F32	29	23	29	34
F16	28	34	33	30	F33	30	32	25	19
F17	2	10	6	6	F34	15	13	14	17

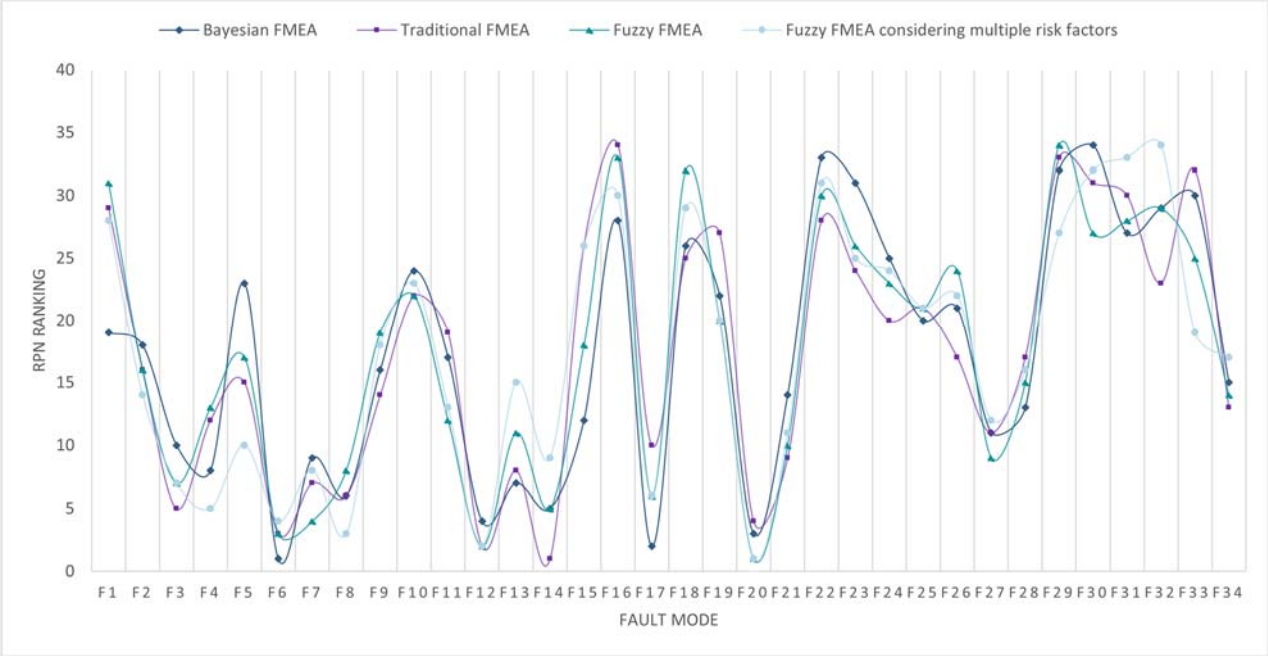

Figure 6. RPN ranking comparison of different FMEAs.

(1) The RPN rankings for eight fault modes (F3, F6, F7, F8, F12, F14, F17, and F20) were higher, with deviations within [0, 5], indicating no significant difference. Conversely, six fault modes (F18, F22, F29, F30, F31, and F32) exhibited relatively low rankings and similar deviations. Notably, 82.4% of the fault modes ranked by the proposed Bayesian FMEA were aligned with those of the other three methods, demonstrating its effectiveness.

(2) In traditional FMEA, fault modes F26 and F28 share the same RPN ranking of 17. In contrast, the proposed Bayesian FMEA assigned RPN rankings of 21 and 13. F26 can effectively stop operations and identify faults, whereas F28 lacks emergency measures and requires testing to diagnose the issues. Thus, F26 exhibited a lower fault risk than F28, which is consistent with the Bayesian FMEA findings. This shows that Bayesian FMEA can better distinguish the fault mode rankings, proving its superiority.

(3) The proposed Bayesian FMEA shows the RPN rankings for fault modes F1, F13, and F15 at 19, 7, and 12, respectively, which significantly exceed 31, 11, and 18 of the fuzzy FMEA, and 28, 15, and 26 of the fuzzy FMEA considering multiple risk factors. This is because F1 and F15 were highly susceptible to various risk factors and other fault modes, whereas F13 could easily affect F7, F8, F9, and F20, potentially causing severe chain reactions. Conversely, the RPN rankings for fault modes F5, F23, and F33 are 23, 31, and 30, respectively, which are lower than 17, 26, and 25 of the fuzzy FMEA and 10, 25, and 19 of the fuzzy FMEA considering multiple risk factors, as these modes do not propagate faults or significantly interact with other risk factors.

Notably, the proposed Bayesian FMEA surpasses traditional and fuzzy FMEAs by more accurately capturing the interactions of risk factors and fault modes, leading to objective and accurate fault risk rankings, and thus proving its superiority.

7. Conclusions

To address the limitations of current studies that focus on individual components without considering fault mode interactions, we propose a Bayesian FMEA method to identify critical fault modes and develop maintenance strategies for stacker-automated stereoscopic warehouses. This method introduces a DSM and hesitant fuzzy expert evaluation to quantify the interactions among fault modes and risk factors. Then, it assesses the fault risks by integrating Bayesian networks and FMEA to identify critical fault modes and their maintenance strategies. Finally, a case study of Company A demonstrates its effectiveness.

(1) The proposed method identifies more potential critical fault modes than Company A, which may not be detectable through expert experience or maintenance manuals and can be easily triggered by risk factors and other faults.

(2) The Bayesian FMEA effectively ranks fault modes, unlike traditional FMEA.

(3) The proposed Bayesian FMEA more accurately reflects fault risk rankings than fuzzy FMEAs by considering the interactions of risk factors and fault modes.

The proposed Bayesian FMEA-based method demonstrates significant effectiveness and practicality in the critical fault identification of stacker-automated stereoscopic warehouses. However, there are still several areas that warrant further exploration:

(1) The weights assigned to the O, S, and D in the current methodology are still based on the assumptions of traditional FMEA, and their relative importance is not fully taken into account. Future research will investigate the relative significance of O, S, and D, aiming to assign dynamic weights to them based on actual data or expert knowledge to enhance the accuracy of critical fault identification.

(2) This method can be applied to complex systems like robotic assembly lines and wind turbines. Expanding its use requires adjustments, such as redefining fault modes and risk factors, gathering specific data, and updating the Bayesian network's conditional probability table. Future research will focus on optimizing the method for diverse systems to enhance its application in complex industrial environments.

Author Contributions: Conceptualization, M.G.; methodology, M.G. and X.M.; software, X.M.; validation, X.M.; formal analysis, M.G. and X.M.; investigation, X.M.; resources, M.G.; data curation, X.M.; writing—original draft preparation, X.M.; writing—review and editing, M.G.; funding acquisition, M.G. All authors have read and agreed to the published version of the manuscript.

Funding: This research was funded by the Science and Technology Planning Project of Zhejiang Provincial Market Supervision Administration, grant number ZD2024005,and the APC was funded by the National Natural Science Foundation of China, grant number 52405569.

Data Availability Statement: The original contributions presented in this study are included in the article. Further inquiries can be directed to the corresponding author.

Conflicts of Interest: The authors declare no conflicts of interest.

Abbreviations

The following abbreviations are used in this manuscript:

FMEA	Failure mode and effects analysis
DSM	Design structure matrix
FTA	Fault tree analysis
ETA	Event tree analysis

GST	Gray system theory
MCS	Monte Carlo simulation
RSM	Risk structure matrix
AHP	Analytic hierarchy process
RPN	Risk priority number
O	Occurrence
S	Severity
D	Detection

Notations

The following notations are used in this manuscript:

r_k	Total background score of the kth expert
ω_k	Background weight of the kth expert
e_{kq}	Evaluation value of the kth expert about the influence between the qth pair of interacting objects
e_q	The qth pair of interacting objects group's weighted average
e_{kq}^{λ}	The λth value in hesitant fuzzy numbers e_{kq}
e_q^{λ}	The λth value in hesitant fuzzy numbers e_q
h	The number of values in one hesitant fuzzy number
d_{kq}	The difference between the evaluation value of the kth expert and the group's weighted average about the influence between the qth pair of interacting objects
H_k	Deviation amount of the kth expert
$f(H_k)$	Standardized deviation amount of the kth expert
T_k	Deviation of the kth expert
$g(T_k)$	Preprocessed deviation of the kth expert
μ_k	Weight influencing factor of the kth expert
$\omega_k^{(p)}$	Final weight of the kth expert is obtained after the pth adjustment
η	The maximum length of all the evaluation sets
$a_{kq\delta}$	The number of δth evaluation levels in the evaluation set of the kth expert on the influence of the qth pair of interacting objects
y_δ	Trapezoidal fuzzy number of the δth evaluation level
w_{ij}	Final influence of the jth evaluation object with the ith evaluation object
BCV_i	Reason vector of the ith evaluation object
BEV_i	Influence vector of the ith evaluation object
CCM_i	Causal interaction comparison matrix of the ith evaluation object
ECM_i	Influence interaction comparison matrix of the ith evaluation object
NCV_i	The maximum eigenvectors of the causal interaction comparison matrices for the ith evaluation object
NEV_i	The maximum eigenvectors of the influence interaction comparison matrices for the ith evaluation object
NCM	Reason matrix
NEM	Influence matrix
RNM	Interaction strength matrix
J_z	The zth node of Bayesian network
E	Directed edge among nodes
L	Conditional probability distributions of nodes
$X(J_z)$	All combinations of parent node states for the zth node
R_n	The nth risk factor
F_m	The mth fault mode
S_u	The uth severity level
D_v	The vth detection level
RPN_m	RPN of the mth fault mode
G	Three-level boundary value

References

1. Li, Z.; Li, M. Design and Implementation of Automated Stereoscopic Warehouse Based on Artificial Intelligence. *Adv. Comput. Commun.* **2023**, *4*, 318–323. [CrossRef]
2. Kuchekar, P.; Bhongade, A.S.; Rehman, A.U.; Mian, S.H. Assessing the Critical Factors Leading to the Failure of the Industrial Pressure Relief Valve Through a Hybrid MCDM-FMEA Approach. *Machines* **2024**, *12*, 820. [CrossRef]
3. Wan, D.; Qiu, H.; Li, M.; Xu, D.; Gao, L. Fuzzy FMEA considering expert consensus and multi-risk factors. *Comput. Integr. Manuf. Syst.* **2024**, 1–22.
4. Li, Y.; Liu, P.; Li, G. An asymmetric cost consensus based failure mode and effect analysis method with personalized risk attitude information. *Reliab. Eng. Syst. Saf.* **2023**, *235*, 109196. [CrossRef]
5. Huang, G.; Xiao, L.; Zhang, G. Risk evaluation model for failure mode and effect analysis using intuitionistic fuzzy rough number approach. *Soft Comput.* **2021**, *25*, 4875–4897. [CrossRef]
6. Skėrė, S.; Bastida-Molina, P.; Hurtado-Pérez, E.; Juzėnas, K. Energy Consumption Analysis and Efficiency Enhancement in Manufacturing Companies Using Decision Support Method for Dynamic Production Planning (DSM DPP) for Solar PV Integration. *Machines* **2023**, *11*, 939. [CrossRef]
7. Babaleye, A.O.; Kurt, R.E.; Khan, F. Safety analysis of plugging and abandonment of oil and gas wells in uncertain conditions with limited data. *Reliab. Eng. Syst. Saf.* **2019**, *188*, 133–141. [CrossRef]
8. Li, S.; Qin, N.; Huang, D.; Huang, D.; Ke, L. Damage localization of stacker's track based on EEMD-EMD and DBSCAN cluster algorithms. *IEEE Trans. Instrum. Meas.* **2019**, *69*, 1981–1992. [CrossRef]
9. Xue, G.; Qiao, Y.; Xia, Y.; Li, Y.; Cheng, Z.; Lei, S.; Wang, L. The development and application of online fault waring system for automatic stereo library based with S7-300 and Wincc flexible 2007 operating environment. In Proceedings of the IEEE 9th International Conference on Mechanical and Intelligent Manufacturing Technologies (ICMIMT), Cape Town, South Africa, 10–13 February 2018.
10. Bao, S.; Zhang, M.; Cai, Z. The slotting optimization of tobacco automated stereoscopic warehouse based on fault tree and field test. In Proceedings of the 2nd IEEE International Conference on Intelligent Transportation Engineering (ICITE), Singapore, 1 September 2019.
11. Tantau, M.; Popp, E.; Perner, L.; Wielitzka, M.; Ortmaier, T. Model selection ensuring practical identifiability for models of electric drives with coupled mechanics. In Proceedings of the 21st IFAC World Congress on Automatic Control—Meeting Societal Challenges, Berlin, Germany, 11–17 July 2020.
12. Zhu, Y.; Xu, B.; Su, J.; Fan, Q.; Miao, J. Fault Diagnosis of AS and RS Based on Fuzzy Petri Net. In Proceedings of the Fault Diagnosis of AS and RS Based on Fuzzy Petri Net, Shanghai, China, 12–15 December 2015.
13. Gnjatovic, N.B.; Urosevic, M.M.; Stefanovic, A.Z.; Bosnjak, S.M.; Zrnic, N.D. Coupled and partial impacts of the inclination angle of the discharge boom and the mass of conveyed material on the dynamic behavior of the stacker superstructure. *Mech. Based Des. Struct. Mach.* **2024**, 1–35. [CrossRef]
14. Bosnjak, S.M.; Arsic, M.A.; Zrnic, N.D.; Odanovic, Z.D.; Dordevic, M.D. Failure Analysis of the Stacker Crawler Chain Link. In Proceedings of the 11th International Conference on the Mechanical Behavior of Materials (ICM), Como, Italy, 5–9 June 2011.
15. Qiao, D.; Zhou, X.; Ye, X.; Tang, G.; Lu, L.; Ou, J. Security risk assessment of submerged floating tunnel based on fault tree and multistate fuzzy Bayesian network. *Ocean Coastal Manage.* **2024**, *258*, 107355. [CrossRef]
16. Maidana, R.G.; Parhizkar, T.; San Martin, G.; Utne, I.B. Dynamic probabilistic risk assessment with K-shortest-paths planning for generating discrete dynamic event trees. *Reliab. Eng. Syst. Saf.* **2024**, *242*, 109725. [CrossRef]
17. Chen, X.; Xu, L.; Li, X.; Cong, L. Risk assessment method of power communication network based on gray cloud theory and matter-element extension model coupling. *IEEE Access* **2023**, *12*, 47581–47593. [CrossRef]
18. Zhang, H.; Sun, J.; Tian, Y. Accelerated risk assessment for highly automated vehicles: Surrogate-based monte carlo method. *IEEE Trans. Intell. Transp. Syst.* **2023**, *25*, 5488–5497. [CrossRef]
19. Zhang, P.; Zhang, Z.; Gong, D. An improved normal wiggly hesitant fuzzy FMEA model and its application to risk assessment of electric bus systems. *Appl. Intell.* **2024**, *54*, 6213–6237. [CrossRef]
20. Min, S.; Jang, H. Case Study of Expected Loss Failure Mode and Effect Analysis Model Based on Maintenance Data. *Appl. Sci.* **2021**, *11*, 7349. [CrossRef]
21. Liu, P.; Xu, Y.; Li, Y.; Geng, Y. An FMEA Risk Assessment Method Based on Social Networks Considering Expert Clustering and Risk Attitudes. *IEEE Trans. Eng. Manage.* **2024**, *71*, 10783–10796. [CrossRef]
22. Huang, W.; Zhang, Y. Railway Dangerous Goods Transportation System Risk Assessment: An Approach Combining FMEA With Pessimistic–Optimistic Fuzzy Information Axiom Considering Acceptable Risk Coefficient. *IEEE Trans. Reliab.* **2021**, *70*, 371–388. [CrossRef]
23. Ustundag, A. A Fuzzy Risk Assessment Model for Warehouse Operations. *J. Mult.-Valued Log. Soft Comput.* **2014**, *22*, 133–149.
24. Li, H.; Zhang, Y.H.; Zheng, Y.; Li, L.H. Research of CBR-Based Organizations on Aromourd Equipment Fault-Diagnosis. *Appl. Mech. Mater.* **2014**, *3485*, 715–721. [CrossRef]

25. Salah, B.; Janeh, O.; Bruckmann, T.; Noche, B. Improving the Performance of a New Storage and Retrieval Machine Based on a Parallel Manipulator Using FMEA Analysis. In Proceedings of the 15th IFAC Symposium on Information Control Problems in Manufacturing, Ottawa, Canada, 11–13 May 2015; pp. 1658–1663.
26. Bevilacqua, M.; Mazzuto, G.; Paciarotti, C. A combined IDEF0 and FMEA approach to healthcare management reengineering. *Int. J. Procure. Manage.* **2015**, *8*, 25–43. [CrossRef]
27. Suwandi, A.; Zagloel, T.Y.; Hidayatno, A. Conceptual model of failure risk control on raw materials inventory system. In Proceedings of the International Conference on Design, Engineering and Computer Sciences (ICDECS), Jakarta, Indonesia, 9 August 2018.
28. Maslowski, D.; Kulinska, E.; Ltd, T. Analysis of the aoolication of FMEA method of warehouse system in metal foundry. In Proceedings of the 27th International Conference on Metallurgy and Materials (METAL), Brno, Czech Republic, 23–25 May 2018; pp. 2036–2041.
29. Hassan, A.; Purnomo, M.R.A.; Anugerah, A.R. Fuzzy-analytical-hierarchy process in failure mode and effect analysis (FMEA) to identify process failure in the warehouse of a cement industry. *J. Eng. Des. Technol.* **2020**, *18*, 378–388. [CrossRef]
30. Dewi, I.L.; Pamadya, V.; Tri, P.A.Y. FMEA Approach to Risk Factors as a Factor in Implementing Green Supply Chain Management (Study in PT. Gresik Cipta Sejahtera). *J. Phys. Conf. Ser.* **2021**, *1858*, 1. [CrossRef]
31. Hsu, H.Y.; Hwang, M.H.; Tsou, P.H. Applications of BWM and GRA for Evaluating the Risk of Picking and Material-Handling Accidents in Warehouse Facilities. *Appl. Sci.* **2023**, *13*, 1263. [CrossRef]
32. Esmaeili, S.V.; Alboghobeish, A.; Yazdani, H.; Koozekonan, A.G.; Pouyakian, M. Optimizing in-store warehouse safety: A DEMATEL approach to comprehensive risk assessment. *PLoS ONE* **2025**, *20*, e0317787. [CrossRef]
33. Huang, X.; Gui, P.; Yao, J.; Zhu, W.; Zhou, C.; Li, X.; Li, S. An Applied View to Determine the Weights of Experts' Scores Based on an Evidential Reasoning Approach Under Two-Dimensional Frameworks. *IAENG Int. J. Comput. Sci.* **2023**, *50*, 970–979.
34. Hernández-Fernández, L.; Vázquez, J.G.; Hernández, L.; Campbell, R.; Martínez, J.; Hajari, E.; González-De Zayas, R.; Zevallos-Bravo, B.E.; Acosta, Y.; Lorenzo, J.C. Use of Euclidean distance to evaluate Pistia stratiotes and Eichhornia crassipes as organic fertilizer amendments in Capsicum annuum. *Acta Physiol. Plant.* **2024**, *46*, 21. [CrossRef]
35. Lu, H.; Bai, Q.; Meng, F. Joint production and sustainability investment decisions for a risk-averse manufacturer under a Cap-and-trade policy. *Sustain. Oper. Comput.* **2024**, *5*, 131–140. [CrossRef]
36. Özdemir, A.; Uçurum, M.; Serencam, H. A novel fuzzy cumulative sum control chart with an α-level cut based on trapezoidal fuzzy numbers for a real case application. *Arab. J. Sci. Eng.* **2024**, *49*, 7507–7525. [CrossRef]
37. Wu, Z.; Li, Y.; Jing, Q. Quantitative risk assessment of coal mine gas explosion based on a Bayesian network and computational fluid dynamics. *Process Saf. Environ. Protect.* **2024**, *190*, 780–793. [CrossRef]
38. Feng, X.; Jiang, J.; Wang, W. Gas pipeline failure evaluation method based on a Noisy-OR gate bayesian network. *J. Loss Prev. Process Ind.* **2020**, *66*, 104175. [CrossRef]
39. Samal, N.; Ashwin, R.; Singhal, A.; Jha, S.K.; Robertson, D.E. Using a Bayesian joint probability approach to improve the skill of medium-range forecasts of the Indian summer monsoon rainfall. *J. Hydrol. Reg. Stud.* **2023**, *45*, 101284. [CrossRef]
40. Zhang, H.; Liu, S.; Dong, Y.; Chiclana, F.; Herrera-Viedma, E.E. A minimum cost consensus-based failure mode and effect analysis framework considering experts' limited compromise and tolerance behaviors. *IEEE T. Cybern.* **2022**, *53*, 6612–6625. [CrossRef] [PubMed]
41. Rakyta, M.; Bubenik, P.; Binasova, V.; Gabajova, G.; Staffenova, K. The Change in Maintenance Strategy on the Efficiency and Quality of the Production System. *Electronics* **2024**, *13*, 3449. [CrossRef]
42. Omshi, E.M.; Shemehsavar, S.; Grall, A. An intelligent maintenance policy for a latent degradation system. *Reliab. Eng. Syst. Saf.* **2024**, *242*, 109739. [CrossRef]
43. Liu, P.; Wang, G.; Tan, Z.-H. Calendar-time-based and age-based maintenance policies with different repair assumptions. *Appl. Math. Model.* **2024**, *129*, 592–611. [CrossRef]
44. Li, X.; Ran, Y.; Fafa, C.; Zhu, X.; Wang, H.; Zhang, G. A maintenance strategy selection method based on cloud DEMATEL-ANP. *Soft Comput.* **2023**, *27*, 18843–18868. [CrossRef]
45. De Jonge, B.; Scarf, P.A. A review on maintenance optimization. *Eur. J. Oper. Res.* **2020**, *285*, 805–824. [CrossRef]
46. Cheikh, K.; Boudi, E.M.; Rabi, R.; Mokhliss, H. Balancing the maintenance strategies to making decisions using Monte Carlo method. *MethodsX* **2024**, *13*, 102819. [CrossRef]
47. Aafif, Y.; Schutz, J.; Dellagi, S.; Chelbi, A.; Mifdal, L. Integrated design and maintenance strategies for wind turbine gearboxes. *J. Qual. Maint. Eng.* **2024**, *30*, 521–539. [CrossRef]
48. Godoy, D.R.; Álvarez, V.; Mena, R.; Viveros, P.; Kristjanpoller, F. Adopting New Machine Learning Approaches on Cox's Partial Likelihood Parameter Estimation for Predictive Maintenance Decisions. *Machines* **2024**, *12*, 60. [CrossRef]
49. Lefebvre, M.; Yaghoubi, R. Optimal Inspection and Maintenance Policy: Integrating a Continuous-Time Markov Chain into a Homing Problem. *Machines* **2024**, *12*, 795. [CrossRef]
50. Esa, M.A.M.; Muhammad, M. Adoption of prescriptive analytics for naval vessels risk-based maintenance: A conceptual framework. *Ocean Eng.* **2023**, *278*, 114409. [CrossRef]

51. Cicek, K.; Celik, M. Application of failure modes and effects analysis to main engine crankcase explosion failure on-board ship. *Saf. Sci.* **2013**, *51*, 6–10. [CrossRef]
52. Kuang, Y.; Zou, S.; Tang, D. Risk analysis for the used or spent fuel shearing machine based on the fuzzy FMEA. *J. Saf. Environ.* **2016**, *16*, 15–20. [CrossRef]

Disclaimer/Publisher's Note: The statements, opinions and data contained in all publications are solely those of the individual author(s) and contributor(s) and not of MDPI and/or the editor(s). MDPI and/or the editor(s) disclaim responsibility for any injury to people or property resulting from any ideas, methods, instructions or products referred to in the content.